Thermalization of mini-jets in a quark-gluon plasma

Edmond Iancu and Bin Wu

Institut de Physique Théorique, CEA Saclay, UMR 3681,
F-91191 Gif-sur-Yvette, France

E-mail: Edmond.Iancu@cea.fr, Bin.Wu@cea.fr

ABSTRACT: We complete the physical picture for the evolution of a high-energy jet propagating through a weakly-coupled quark-gluon plasma by investigating the thermalization of the soft components of the jet. We argue that the following scenario should hold: the leading particle emits a significant number of mini-jets which promptly evolve via quasi-democratic branchings and thus degrade into a myriad of soft gluons, with energies of the order of the medium temperature T. Via elastic collisions with the medium constituents, these soft gluons relax to local thermal equilibrium with the plasma over a time scale which is considerably shorter than the typical lifetime of the mini-jet. The thermalized gluons form a tail which lags behind the hard components of the jet. We support this scenario, first, via parametric arguments and, next, by studying a simplified kinetic equation, which describes the jet dynamics in longitudinal phase-space. We solve the kinetic equation using both (semi-)analytical and numerical methods. In particular, we obtain the first exact, analytic, solutions to the ultrarelativistic Fokker-Planck equation in one-dimensional phase-space. Our results confirm the physical picture aforementioned and demonstrate the quenching of the jet via multiple branching followed by the thermalization of the soft gluons in the cascades.

Contents

1   Introduction

It is by now well established that, within weakly-coupled QCD at least, the energy loss by an energetic parton and/or the associated jet propagating through a dense medium, such as a quark-gluon plasma, is dominated by *medium-induced radiation*, that is, the additional radiation triggered by the interactions between the partons from the jet and the medium constituents [1–11] (see also the review papers [12–14]). This picture has led to a rather successful phenomenology, based on, or at least inspired by, calculations in perturbative QCD, which has allowed one to understand many interesting observables at RHIC and the LHC, like the nuclear modification factor or the suppression of di-hadron azimuthal correlations in ultrarelativistic nucleus-nucleus collisions [15–18].

    More recently, the experimental studies of the phenomenon known as 'di-jet asymmetry' in Pb+Pb collisions at the LHC have demonstrated that a substantial fraction of the energy loss by an energetic jet is carried by relatively soft hadrons propagating at large angles with respect to the jet axis [19–26]. This pattern too can be understood, at least

qualitatively, within the pQCD picture for medium-induced radiation, which predicts the formation of well-developed gluon cascades, or 'mini-jets', via multiple branching [27–35] (see also refs. [36–39] for earlier, related, studies and the recent review paper [40]). Within these cascades, the energy is efficiently transmitted, via quasi-democratic branchings, from the 'leading particle' — the parton that has initiated the jet — to a large number of comparatively soft gluons, which can be easily deviated towards large angles by rescattering in the medium. The theoretical description of medium-induced multiple branching started being developed only recently and in its current formulation it leaves unanswered a number of important questions, among which: what is the physical mechanism which *stops* the medium-induced cascades, and at which energy scale? How does this mechanism influence the dynamics of the branchings (in particular, the gluon spectrum) at *higher* energy scales? What is the fate of the softest quanta, as produced at the *low-energy end* of the cascade? What is the precise mechanism for energy transfer from the jet to the medium and what are the imprints of this transfer on the medium itself?

We shall focus on high-energy jets, as relevant for the LHC: the original energy E of the leading particle is assumed to be much larger than the characteristic energy scale of the medium — the temperature T for the case of a quark-gluon plasma in thermal equilibrium, or, more generally, the average p_T of the background hadrons. Then the parton cascades produced via successive branchings are themselves dominated by *hard* gluons, with energies $\omega \gg T$, whose emissions are controlled by the BDMPSZ mechanism[1] [2–5], that is, by multiple soft scattering in the medium. A distinguished feature of this mechanism is that it favors 'quasi-democratic branchings' [28, 36, 41], leading to a phenomenon of *wave turbulence* [28]: via successive splittings, the energy flows from one parton generation to the next one, without accumulating at any intermediate step (see section 2 below for details).

In most theoretical analyses so far, on has assumed that this 'ideal' (or 'turbulent') branching dynamics remains unmodified down to arbitrarily low energies. This simplification allowed for exact solutions [28, 30, 35], which exhibit a characteristic *scaling spectrum* — the Kolmogorov-Zakharov spectrum of wave turbulence [42, 43]. But this 'ideal' scenario also leads to some unphysical predictions: after a finite interval of time, the original energy E gets transmitted to an infinite number of arbitrarily soft quanta, which form a 'condensate' at $\omega = 0$. This result is unphysical in that it violates a basic assumption underlying the linear dynamics studied in [28, 30, 35] — the fact that the gluon occupation numbers are supposed to be small. It also contradicts our physical expectation that the relatively soft gluons with $\omega \lesssim T$ should *thermalize*, via collisions in the plasma, and thus decouple from the cascades.

A proper treatment of the dynamics at the 'soft' scale $\omega \sim T$ is necessary not only to understand the energy transfer between the jet and the medium, but also to assess the validity of the 'ideal branching' picture at higher energies $\omega \gg T$. Indeed, the physics of wave turbulence is very sensitive to the details of the mechanism for energy absorption at the low-energy end of the cascade [42, 43]. A power-law spectrum of the Kolmogorov-Zakharov type can develop only in the presence of a *perfect sink* — a mechanism which absorbs the energy flux carried by the cascade at some scale p_*, without affecting the

---

[1]The acronym 'BDMPSZ' stands for Baier, Dokshitzer, Mueller, Peigné, Schiff, and Zakharov.

branching dynamics at higher energies $\omega \gg p_*$. For the jet problem at hand, one expects the medium to act as an energy absorber at $p^* \sim T$, but it is not clear whether this absorber qualifies as a 'perfect sink', not even approximately. In fact, an attempt to mimic thermalization by introducing an 'infrared' cutoff p_* in the branching rate resulted in a strong distortion of the scaling spectrum up to very high energies $\omega \gg p_*$, due to the accumulation of gluons in the bins above p_* ('pile-up') [32]. Without a detailed study of thermalization, it seems difficult to decide whether this pile-up is a genuine physical phenomenon, or merely an artifact of the prescription used to terminate the cascade.

It is our main purpose in this paper to provide an explicit study of the thermalization of the soft components of the jet, under the assumption that the medium is a weakly-coupled quark-gluon plasma with temperature T. To that aim, we shall consider a special kinetic equation, which emerges via controlled approximations from more general (but also more difficult to solve) equations in the literature [36, 44], and which captures the interesting dynamics to parametric accuracy. This equation, to be introduced in section 3, describes the evolution of the gluon distribution $f(t, z, p_z)$ created by the jet in the longitudinal phase-space, that is, along the direction of propagation of the leading particle. The restriction to the longitudinal dynamics is needed to simplify the problem, but it is also physically motivated: the longitudinal momenta of the gluons within the cascade remain much larger than the respective transverse components ($p_z \gg p_\perp$) so long as $\omega \gg T$, that is, during most stages of the branchings process, hence they control the relevant time scales.

The kinetic equation includes two collision terms: an inelastic one, describing multiple branching with the BDMPSZ splitting rate, and an elastic one, which describes $2 \to 2$ collisions with the medium constituents in the Fokker-Planck approximation [45]. The latter is traditionally employed for 'test particles' which can be distinguished from the thermal bath (like a heavy quark [46, 47]), but can also be applied to the gluons from the jet with relatively large momenta $p_z \simeq \omega \gg T$ [48].

On the other hand, our equation becomes inaccurate for softer energies $\omega \lesssim T$, where, besides the transverse dynamics, it also misses non-linear phenomena, like the $2 \to 1$ gluon recombination, which are expected to stop the branching dynamics in the approach towards thermal equilibrium [36, 44, 48, 53]. In practice, we shall mimic these non-linear effects by inserting an 'infrared' cutoff $p_* \sim T$ in the splitting rate. This prescription is indeed justified in our present set-up because of the simultaneous inclusion of the elastic collisions, which smear out the effects of the cutoff and thus remove, or at least reduce, potential artifacts like the 'pile-up'. Still because of the linearization, our approximation misses the effects of the quantum, Bose-Einstein, statistics; accordingly, it describes thermalization as the approach towards a classical thermal distribution (for ultrarelativistic particles), of the Maxwell-Boltzmann type.

In sections 4 and 5, we shall study the kinetic equation via a combination of (semi)analytic and numerical methods. For the Fokker-Planck dynamics alone, we shall construct exact, analytic, solutions, including the exact Green's function in longitudinal phase-space (see section 4.2.1). By combining this Green's function with the known analytic solutions for the ideal branching process [28, 30, 35], we shall provide a first, and relatively simple, discussion of the complete dynamics, under the assumption that the medium acts as a 'perfect sink' (see section 4.2.2).
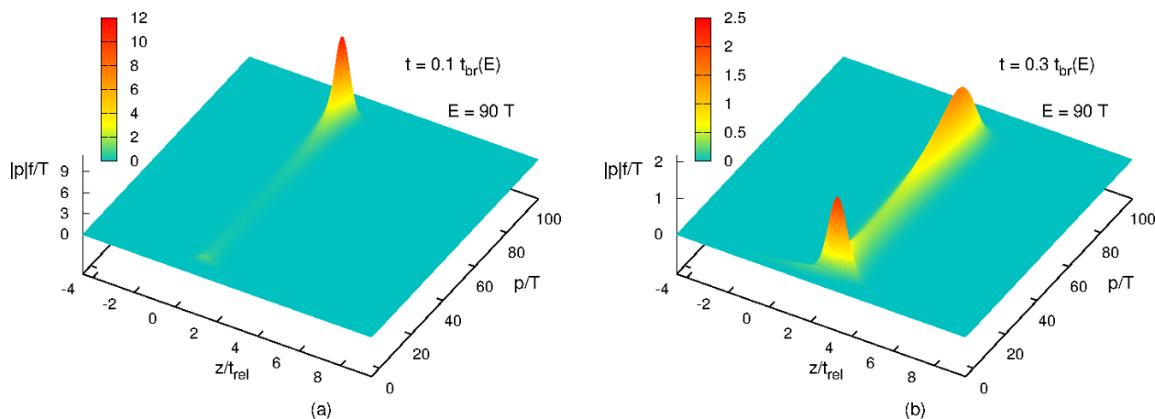
Figure 1. The phase-space energy density $|p|f/T$ produced by an energetic jet with $E = 90\,T$ at two successive times: (a) an early time $t = 0.1t_{\mathrm{br}}(E)$, when the jet is almost unquenched; (b) a larger time $t = 0.3t_{\mathrm{br}}(E)$, when the jet is partially quenched. The secondary peak visible around $p \sim T$ in plot (b) represents the energy lost towards the medium via thermalization. The reference scale $t_{\mathrm{br}}(E) \sim (1/\alpha_s)\sqrt{E/\hat{q}}$ is the typical time it would take the LP with energy E to undergo a democratic branching (see section 2.1 for details).

Section 5 presents a detailed numerical analysis of the kinetic equation, with conclusions which corroborate and complete the general physical discussion in section 2, as well as the semi-analytic studies in section 4. The physical picture which emerges from these studies is summarized in what follows.

An energetic leading particle (LP) with $E \gg T$ emits a significant number of primary gluons, with energies in the range $T \ll \omega \ll E$. In turn, each of these primary gluons gives rise to a gluon cascade, or 'mini-jet', via successive democratic branchings and thus transmits its whole initial energy ω to a large number $N \sim \omega/T$ of soft gluons, with energies of order T. The typical lifetime of such a mini-jet is $t_{\mathrm{br}}(\omega) \sim (1/\alpha_s)\sqrt{\omega/\hat{q}}$, with $\hat{q}$ the jet quenching parameter. Finally, these soft gluons thermalize via elastic collisions, during a typical time $t_{\mathrm{rel}} \sim 1/[\alpha_s^2 \ln(1/\alpha_s)]$ which is much shorter than $t_{\mathrm{br}}(\omega)$ so long as $\omega \gg T$. This dynamics generates a characteristic jet structure in the longitudinal phase-space, which involves two components: the 'front' and the 'tail'.

The 'front' is made with relatively hard gluons, with $p_z \gg T$, which are localized near $z = t$ and which are distributed in p_z according to the scaling spectrum (with only a small distortion due to pile-up); that is, the front looks very much like a jet that would be produced by 'ideal branching'. The 'tail' lags behind the front, at $z < t$, and is made with thermalized gluons; the corresponding distribution $f(t, z, p_z)$ is proportional to $\mathrm{e}^{-|p_z|/T}$ and smoothly decreases with $t - z$. The energy carried by the gluons in this thermalized tail is naturally interpreted as the *energy lost by the jet to the medium*. This is controlled by the hardest 'mini-jets', those with energies $\omega \sim \alpha_s^2 \hat{q} L^2$, where L is the length of the medium as crossed by the LP. Hence, the energy loss scales like the medium size squared.

More precisely, this picture holds provided the LP particle is energetic enough for $t_{\mathrm{br}}(E) \gg L$. As we shall argue, this is indeed the typical situation for the jet kinematics at the LHC. In figure 1, we show the jet distribution emerging from our calculations at two

successive times. At the very early time $t = 0.1 t_{\rm br}(E)$, most of the energy is still carried by the LP and the tail is not yet visible. This situation is illustrative for the 'trigger' (or 'leading') jet in the phenomenology of di-jet asymmetry, which crosses at most a very narrow slab of matter. At the larger time $t = 0.3 t_{\rm br}(E)$, the LP peak is still visible, but a substantial fraction of the initial energy E has been transferred to the front and the thermalized tail. This situation, where the jet looks partially quenched, is representative for the 'away' (or 'subleading') jet in a di-jet event characterized by a large asymmetry. For even larger times, $t \gtrsim t_{\rm br}(E)$, both the LP and the front would disappear and the whole energy would be found in the thermalized tail (see the discussion in section 5). However, this complete quenching scenario cannot occur for the very energetic jets with $E \geq 100\,{\rm GeV}$ that are measured at the LHC.

2 The physical picture

In this section, we summarize the physical picture underlying the in-medium evolution of a jet generated by a high-energy parton propagating through a weakly-coupled quark-gluon plasma. This picture largely reflects the current understanding of this problem, as presented in the literature, but includes some additional arguments which are physically motivated and which will be later on confirmed by the new analysis in this work. We start with a brief review of recent studies of the medium-induced gluon cascade [27–30], which recognized the importance of multiple branchings, but did not address the important problem of the thermalization of the soft components of the jet. Then we discuss the interplay between multiple branching and the elastic collisions responsible for thermalization.

2.1 Inelastic collisions: jet evolution via multiple branching

An energetic 'probe' parton (gluon or quark) which propagates through a dense QCD medium, such as a quark-gluon plasma, undergoes elastic collisions with the constituents of the medium, leading to 'collisional' energy loss and to the broadening of the probe distribution in (longitudinal and transverse) momentum, due to the random nature of the 'kicks'. Besides, the collisions trigger gluon emissions by the probe, leading to additional, 'radiative', energy loss, which in practice dominates over the collisional one, in spite of the fact that the emission probability is suppressed by a factor of α_s. This is possible because the coherence effects inherent in a quantum emission lead to a stronger dependence of the energy loss upon the medium size — the radiative component rises, roughly, like L^2 (with L the distance traveled by the probe through the medium), whereas the collisional component rises only like L. Notwithstanding, the elastic collisions will play an important role in the subsequent discussion.

The precise mechanism responsible for medium-induced radiation depends upon the ratio between the gluon 'formation time' $t_{\rm form} \sim \omega/p_\perp^2$ (the typical time it takes to radiate a gluon with energy ω and transverse momentum $p_\perp$) and the mean free path $\lambda_{\rm mfp} \sim 1/[\alpha_s T \ln(1/\alpha_s)]$ between two successive small-angle collisions. For a single collision, one has $p_\perp^2 \sim m_D^2 \sim \alpha_s T^2$, with m_D the Debye mass. For a series of independent collisions occurring during a time interval $\Delta t \gg \lambda_{\rm mfp}$, one has $p_\perp^2 \sim \hat{q} \Delta t$, where $\hat{q} \simeq m_D^2/\lambda_{\rm mfp} \sim$

$\alpha^2 T^3 \ln(1/\alpha_s)$ is the jet quenching parameter. With increasing ω, one interpolates between a single-scattering (or 'Bethe-Heitler') regime at low energies $\omega \lesssim T$, where $t_{\rm form} \sim \omega/m_D^2 \lesssim \lambda_{\rm mfp}$, and a multiple-scattering (or 'LPM', from Landau, Pomeranchuk, and Migdal) regime at high energies $\omega \gg T$, where $t_{\rm form} \sim \sqrt{\omega/\hat{q}} \gg \lambda_{\rm mfp}$. The typical elementary processes are $2 \to 3$ collisions in the Bethe-Heitler regime and, respectively, $1+({\rm many}) \to 2+({\rm many})$ collisions in the LPM regime.

In what follows, we shall consider the LPM regime alone. Indeed, we shall later argue that the branching process terminates around $\omega \sim T$, hence the phase-space for Bethe-Heitler radiation is comparatively small. The calculation of the gluon branching rate in the LPM regime to leading order in pQCD has been first given by Baier, Dokshitzer, Mueller, Peigné, and Schiff [2, 3, 6], and independently by Zakharov [4, 5]. One has thus obtained the following result for the differential probability per unit time and per unit x for the collinear splitting[2] of a gluon with energy ω into two daughter gluons with energy fractions x and $1-x$, with $0 < x < 1$:

$$\frac{{\rm d}^2 \mathcal{I}_{\rm br}}{{\rm d}x\, {\rm d}t} = \frac{\alpha_s}{2\pi} \frac{P_{g \to g}(x)}{t_{\rm form}(x, \omega)}\,. \tag{2.1}$$

In this equation, $P_{g \to g}(x) = N_c[1 - x(1-x)]^2/x(1-x)$, with N_c the number of colors, is the leading order gluon-gluon splitting function of the DGLAP equation and $t_{\rm form}(x, \omega)$ is a more precise estimate for the formation time, which involves the average energy $x(1-x)\omega$ of the two daughter gluons:

$$t_{\rm form}(x, \omega) \equiv \sqrt{\frac{x(1-x)\omega}{\hat{q}_{\rm eff}(x)}}\,, \qquad \hat{q}_{\rm eff}(x) \equiv \hat{q}\,[1 - x(1-x)]\,. \tag{2.2}$$

Using eq. (2.1), one can evaluate the probability for a branching to occur during a given interval Δt:

$$\Delta \mathcal{P} \simeq x \frac{{\rm d}^2 \mathcal{I}_{\rm br}}{{\rm d}x\, {\rm d}t} \Delta t \sim \bar{\alpha} \sqrt{\frac{\hat{q}}{x(1-x)\omega}} \Delta t\,, \tag{2.3}$$

where $\bar{\alpha} \equiv \alpha_s N_c/\pi$. This probability becomes of order one, meaning that multiple branching is important during Δt, provided

$$x(1-x)\omega \sim \bar{\alpha}^2 \hat{q} \Delta t^2 \equiv \omega_{\rm br}(\Delta t)\,. \tag{2.4}$$

This condition can be satisfied by two types of emissions:

(a) very asymmetric splittings, for which either $x \ll 1$ or $1-x \ll 1$, whereas the energy ω of the parent gluon can be relatively hard (for instance, $\omega \gg \omega_{\rm br}(\Delta t)$);

(b) 'quasi-democratic' branchings, where the two daughter gluons carry comparable fractions of the total energy, $x \sim 1-x \sim \mathcal{O}(1)$, but the parent gluon is relatively soft: $\omega \sim \omega_{\rm br}(\Delta t)$.

---

[2]The splitting is effectively collinear since the transverse momentum squared acquired by the gluon during the formation time $t_{\rm form}$ is much smaller than the respective quantity acquired after formation, namely during the lifetime $t_{\rm br} \sim t_{\rm form}/\bar{\alpha}$ of the gluon until its next splitting (see below).

Reversing the argument for case (b) above, we conclude that it takes a time $\Delta t \sim t_{\rm br}(\omega)$, with

$$t_{\rm br}(\omega) \equiv \frac{1}{\bar{\alpha}} \sqrt{\frac{\omega}{\hat{q}}}, \qquad (2.5)$$

for a gluon with energy ω to undergo a 'quasi-democratic' branching [28, 36, 41]. This duration $t_{\rm br}(\omega)$ should be compared to the medium size L which is available to that parton:

(i) If $t_{\rm br}(\omega) \gg L$, then the parton with energy ω can emit *abundantly* — i.e. with probability of $\mathcal{O}(1)$ — only relatively soft gluons with $x \ll 1$, such that $x\omega \lesssim \omega_{\rm br}(L) = \bar{\alpha}^2 \hat{q} L^2$. Accordingly, the original parton will 'survive the medium': it will be recognizable in the final state since much more energetic than its products of radiation.

(ii) If $t_{\rm br}(\omega) \lesssim L$, then the parton with energy ω will 'disappear inside the medium' — it will undergo a quasi-democratic branching before exiting the medium, and its daughter gluons will typically split again and again, thus eventually producing a gluon cascade. Each new gluon generation in this cascade has a lower energy and hence a shorter lifetime than the previous ones. Accordingly, the overall lifetime of the cascade is of the order of the branching time $t_{\rm br}(\omega)$ of the initial gluon.

Case (i) is the interesting situation for the leading particle (LP) which initiates a typical jet measured in Pb+Pb collisions at the LHC. Indeed, this LP has an energy $E \geq 100\,{\rm GeV}$, which is much larger than the characteristic energy for multiple branching within a typical medium size L: $\omega_{\rm br}(L) = \bar{\alpha}^2 \hat{q} L^2 \simeq 12\,{\rm GeV}$ for a medium with $\hat{q} = 1{\rm GeV}^2/{\rm fm}$ and $L = 5\,{\rm fm}$ (we used $\bar{\alpha} = 0.3$). The above estimate also shows that, for the interesting values of L, the branching scale $\omega_{\rm br}(L)$ is much harder than the medium temperature $T \simeq 0.5\,{\rm GeV}$; hence, one typically has $T \ll \omega_{\rm br}(L) \ll E$.

Case (ii) applies to the *typical* primary gluons — the gluons which are directly radiated by the LP in a typical event. Indeed, such gluon have relatively soft energies $\omega \lesssim \omega_{\rm br}(L)$ and therefore they split fast enough to develop gluon cascades ('mini-jets') via quasi-democratic branchings. Harder primary emissions, with energies up to[3] $\omega_c \equiv \hat{q} L^2$, are possible as well (provided $E > \omega_c$, of course), but these are rare events which occur with a probability of $\mathcal{O}(\bar{\alpha})$ and do not generate mini-jets. Such hard but rare emissions will therefore not be explicitly considered in what follows.

The quasi-democratic nature of the splittings leads to *wave turbulence* [28, 30]: via successive branchings, the energy flows from one gluon generation to the next one, without accumulating at any intermediate value of ω. The precise criterion for wave turbulence is that the energy flux — the rate for energy flow along the cascade — be independent of ω (see section 4.2.2 below for details).

If this branching dynamics was to remain unmodified down to arbitrarily small values of ω, then the whole energy would end up into a 'condensate' at $\omega = 0$ [28]. In reality though, we expect the gluon cascade to terminate at the thermal scale T, because the very soft quanta with $\omega \lesssim T$ can efficiently thermalize via elastic collisions (see section 2.2

---

[3]This upper limit ω_c on the energy of medium-induced gluon emissions follows from the condition that the gluon formation time $t_{\rm form}(\omega)$ be at most as large as L.

below). If the medium acts as a *perfect sink* at the lower end of the cascade — in the sense of absorbing all the quanta with $\omega \lesssim T$ without modifying the dynamics of branching at higher energies $\omega \gg T$ — then the whole energy carried by the turbulent flow is eventually transmitted to the medium. Under this assumption, the energy lost by the jet towards the medium is obtained as [28, 30]

$$\Delta E_{\text{flow}} \simeq \frac{\upsilon}{2}\, \omega_{\text{br}}(L) = \frac{\upsilon}{2}\, \bar{\alpha}^2 \hat{q} L^2 \,, \tag{2.6}$$

with $\upsilon \simeq 4.96$. This result, which is independent of the initial energy E of the LP and grows with the medium size like L^2, truly applies (under the 'perfect sink' assumption) for a very energetic jet with $E \gg \omega_{\text{br}}(L)$. In the opposite limit where $E \lesssim \omega_{\text{br}}(L)$ (the case of a mini-jet), one rather has $\Delta E_{\text{flow}} \simeq E$ (see eq. (4.30) for a more general expression). We shall later discover that the assumption that the medium acts as a 'perfect sink' has some limitations in practice, yet it can be used for qualitative considerations and parametric estimates.

Another important assumption that was implicitly postulated by previous analyses of multiple branching [28, 30] is that the branching dynamics is *linear*, meaning that the gluons from the cascade can split, but not also recombine with each other. This assumption is correct provided the partons cascade are sufficiently dilute. The precise condition is that $f(t, \boldsymbol{x}, \boldsymbol{p}) \ll 1$, where $f(t, \boldsymbol{x}, \boldsymbol{p})$ is the *gluon phase-space occupation number* (below, N_g is the total number of gluons in the jet),

$$f(t, \boldsymbol{x}, \boldsymbol{p}) \equiv \frac{(2\pi)^3}{2(N_c^2 - 1)} \frac{\mathrm{d}N_g}{\mathrm{d}^3\boldsymbol{x}\mathrm{d}^3\boldsymbol{p}} \,. \tag{2.7}$$

This quantity has not been explicitly computed in the previous studies, but it is straightforward to obtain an order-of-magnitude estimate for it via physical considerations.

Consider a typical mini-jet, as generated by a primary gluon with initial energy $\omega_0 \lesssim \omega_{\text{br}}(L)$. Over a time interval of order $t_{\text{br}}(\omega_0)$, this whole energy gets redistributed, via multiple branching, among a large number $N_g \simeq \omega_0/T$ of soft quanta with energies $\omega \sim T$. Their occupancy can therefore be estimated as

$$f(T) \sim \frac{1}{N_c^2} \frac{\omega_0/T}{p_z \Delta z\, \Delta p_\perp^2 \Delta x_\perp^2} \,, \tag{2.8}$$

where $p_z \sim \omega \sim T$, $\Delta p_\perp^2$ is the transverse momentum squared acquired by a gluon via rescattering in the medium, Δz is the longitudinal extent of the distribution, and $\Delta x_\perp^2$ is the corresponding spread in the transverse plane.

The transverse phase-space $\Delta p_\perp^2 \Delta x_\perp^2$ occupied by a gluon with energy $\omega \sim p_z$ turns out to be independent of ω. Indeed, during a time Δt, a gluon accumulates a transverse momentum broadening $\Delta p_\perp^2 \simeq \hat{q}\Delta t$, leading to an uncertainty

$$\Delta x_\perp^2 \simeq \frac{\Delta p_\perp^2}{p_z^2}\, \Delta t^2 \simeq \frac{\hat{q}\Delta t^3}{\omega^2} \tag{2.9}$$

in its transverse location. Taking Δt of the order of the gluon lifetime, $\Delta t \sim t_{\text{br}}(\omega)$, one finds

$$\Delta p_\perp^2 \, \Delta x_\perp^2 \simeq \left(\frac{\hat{q}\, t_{\text{br}}^2(\omega)}{\omega} \right)^2 \sim \frac{1}{\bar{\alpha}^4} \,. \tag{2.10}$$

This is independent of ω, as anticipated, and parametrically large. The above argument also shows that, so long as $\omega \gg T$, the transverse momenta of the gluon produced by the branching process remain much smaller than the longitudinal ones: $p_\perp \ll p_z \simeq \omega$.

Consider now the longitudinal distribution of the soft quanta within the mini-jet. As already discussed, soft gluons are emitted promptly, so they can be produced anywhere along the cascade. After being emitted, they efficiently lose energy and randomize their direction of motion, via elastic collisions. Accordingly, they remain behind the harder ($p \gg T$) partons in the mini-jet, which still propagate at the speed of light and form the jet front (see the discussion in section 4.1). Thus, on the average, the soft gluons are quasi-uniformly distributed along z, within a distance $\Delta z \sim t_{\mathrm{br}}(\omega_0)$ behind the front at $z \simeq t$. Using this, together with (2.8) and (2.10), we finally deduce

$$ f(T) \sim \frac{\bar{\alpha}^4}{N_c^2} \frac{\omega_0}{T^2 t_{\mathrm{br}}(\omega_0)} \,. \tag{2.11} $$

This number increases with ω_0, so it is interesting to evaluate it for the hardest mini jets, those with $\omega_0 \sim \omega_{\mathrm{br}}(L)$. In that case, $t_{\mathrm{br}}(\omega_0) \simeq L$, hence

$$ f(T) \sim \frac{\bar{\alpha}^6}{N_c^2} \frac{\hat{q}L}{T^2} \,. \tag{2.12} $$

This result has been obtained here for a mini-jet, but the corresponding estimate for the jet as a whole is roughly larger by a factor $\upsilon \simeq 4.96$, cf. eq. (2.6). The occupation number (2.12) is parametrically small at weak coupling and furthermore suppressed at large N_c. It is easy to check that the condition $f(T) \ll 1$ is always very well satisfied in practice.

The estimate in eq. (2.12) should be truly viewed as a *lower* limit on f: as we shall explain in section 4.2.2, the soft gluons with $\omega \sim T$ are more abundantly produced during the late stages of the cascade, at times $t \sim t_{\mathrm{br}}(\omega_0)$, so their distribution in z is not really homogeneous. (This will be also confirmed by the numerical simulations in section 5; see figure 8.) An *upper* limit on $f(T)$ can be obtained by assuming the smallest possible longitudinal spread for the soft gluons, namely their lifetime $t_{\mathrm{br}}(T) \sim 1/\bar{\alpha}^2 T$. With $\Delta z \sim t_{\mathrm{br}}(T)$ and $\omega_0 \sim \omega_{\mathrm{br}}(L)$, eq. (2.8) implies,

$$ f(T) \sim \frac{\bar{\alpha}^4}{N_c^2} \frac{\omega_{\mathrm{br}}(L)}{T^2 t_{\mathrm{br}}(T)} \sim \frac{\bar{\alpha}^8}{N_c^2} \frac{\hat{q}L^2}{T} \,, \tag{2.13} $$

which is still much smaller than one in all practical situations of interest, as one can easily check.

As it should be clear from the previous discussion, the above estimates for f refer exclusively to the soft gluons generated by the jet via multiple branching. When $\omega \sim T$, these gluons add to those from the background medium, whose occupation numbers are given by the usual, Bose-Einstein, thermal distribution and hence are of order one. So the present results also show that the effect of the jet on the occupancy of gluons with $\omega \lesssim T$ represents only a small perturbation: the jet cannot produce 'hot spots' in the medium (it cannot significantly increase the local energy density).

2.2 Elastic collisions and thermalization

In the previous discussion, the medium constituents had merely the role to trigger gluon emissions via inelastic collisions with the partons from the jet. But the elastic, $2 \to 2$, collisions can be important as well, in that they lead to collisional energy loss and momentum broadening for the jet constituents. As we shall explain in what follows, these additional effects are negligible for the relatively hard gluons with $\omega \gg T$, but they become important for the softer gluons with $\omega \sim T$, which can thermalize via elastic collisions in the medium.

To study the effects of the elastic collisions, we shall employ the Langevin (or Fokker-Planck) approach, which has the advantage of simplicity (see e.g. [45–48] for more details on this formalism). This formalism is *a priori* justified for small angle scatterings and for 'test' particles, like a heavy quark, which can be unambiguously distinguished from the thermal particles. For the jet problem at hand, it strictly applies for the hard gluons with $\omega \gg T$, but it can also be used for studies of thermalization to parametric accuracy.

For more clarity, let us first assume that the branching dynamics is switched off and focus on an energetic, 'test', particle which suffers elastic collisions in the plasma. The Langevin equation reads[4]

$$\frac{\mathrm{d}p^i}{\mathrm{d}t} = -\eta v^i + \xi^i, \qquad \langle \xi^i(t)\xi^j(t')\rangle = \frac{\hat{q}}{2}\,\delta^{ij}\delta(t-t')\,, \tag{2.14}$$

where $v^i = p^i/p$, with $i = 1, 2, 3$, is the particle velocity, η is a friction coefficient, and ξ^i is a stochastic force (the 'noise'). Microscopically, the total force in the r.h.s. of eq. (2.14) represents the Lorentz force due to the color fields of the thermal particles, which are slightly disturbed out-of-equilibrium by their scattering off the probe particle. The 'drag force' $f^i = -\eta v^i$ describes the average effect of this microscopic force, which is the energy transfer from the probe to the medium, whereas the noise term ξ^i represents its random component leading to momentum broadening (or 'diffusion'). The average over the noise reflects the thermal average over the microscopic sources of this force.

By using a properly discretized version of the stochastic equation (2.14) (see e.g. [46]), one can deduce the following evolution equation for the average of the particle momentum squared:

$$\frac{\mathrm{d}\langle p^2 \rangle}{\mathrm{d}t} = -2\eta\langle p\rangle + \frac{3}{2}\hat{q}\,. \tag{2.15}$$

For this equation to be consistent with the approach towards the thermal distribution[5] $f_p \propto \mathrm{e}^{-p/T}$ (which in turn implies $\langle p \rangle = 3T$ and $\langle p^2 \rangle = 12T^2$), one needs the Einstein

---

[4]In general, $(\hat{q}/2)\delta^{ij}$ in the r.h.s. of the noise correlator gets replaced by $\hat{q}^{ij} = \hat{q}_\ell \hat{v}^i \hat{v}^j + (\hat{q}/2)(\delta^{ij} - \hat{v}^i \hat{v}^j)$, where the longitudinal ($\hat{q}_\ell$) and transverse ($\hat{q}$) momentum diffusion coefficients are different from each other. But for a massless energetic particle and in the lowest, leading-logarithmic, approximation it so happens that $\hat{q}_\ell = \hat{q}/2$; see e.g. [46, 48, 49].

[5]The probe gluon is here treated as a classical particle, hence its momentum distribution in thermal equilibrium is the relativistic version of the classical Maxwell-Boltzmann distribution, also known as the Maxwell-Jüttner distribution.

relation $\hat{q} = 4T\eta$ between diffusion and drag. This is guaranteed by the fluctuation-dissipation theorem for thermal correlations.

Assume that the test particle enters the medium at $t = 0$ with a large momentum $p_0 \gg T$ oriented along the z axis ($i = 3$): $v_z \equiv v^3 = 1$. At early stages, the effects of diffusion are negligible ($p_\perp \ll p_z$), and by taking the average in the Langevin equation one finds $\langle p_z(t) \rangle \simeq p_0 - \eta t$. This implies that the particle loses most of its energy, from the initial value $p_0 \gg T$ down to a value $p \sim T$ where diffusion starts to be important, over an interval $\Delta t \simeq p_0/\eta = (p_0/T)t_{\rm rel}$, with

$$ t_{\rm rel} \equiv \frac{4T^2}{\hat{q}} \sim \frac{1}{\bar{\alpha}^2 T \ln(1/\bar{\alpha})} \,. \tag{2.16} $$

From that moment on, the particle approaches the thermal distribution quite fast, over a time $\Delta t \sim t_{\rm rel}$, under the combined effect of drag and diffusion. This can be understood from the fact that its momentum broadening increases with time like $\langle p^2 \rangle \simeq (3/2)\hat{q}\Delta t$, cf. eq. (2.15), and hence it becomes of $\mathcal{O}(T^2)$ after a time $\Delta t \sim T^2/\hat{q} \sim t_{\rm rel}$. Clearly, when $p_0 \gg T$, the total duration of the thermalization process is controlled by the first period — the energy loss via drag — and is of order $t_{\rm drag}(p_0)$, with

$$ t_{\rm drag}(p) \equiv \frac{p}{T}\, t_{\rm rel} = \frac{4pT}{\hat{q}} \,. \tag{2.17} $$

Let us now return to our jet problem and switch on the branching dynamics, on top of the elastic collisions. From the previous subsection, we know that a primary gluon with energy $p_0 \gg T$ has a lifetime $\Delta t \sim t_{\rm br}(p_0)$ before it undergoes a first democratic branching. By comparing eqs. (2.5), (2.16), and (2.17), it is clear that the following hierarchy holds among the relevant time scales:

$$ t_{\rm drag}(p) \gg t_{\rm br}(p) \gg t_{\rm rel} \qquad \text{for} \qquad p \gg T \,. \tag{2.18} $$

Indeed, by using $\hat{q} \sim \bar{\alpha}^2 T^3$ for the weakly-coupled QGP, one deduces

$$ \frac{t_{\rm br}(p)}{t_{\rm drag}(p)} = \frac{1}{4\bar{\alpha}}\sqrt{\frac{\hat{q}}{pT^2}} \sim \sqrt{\frac{T}{p}} \,. \tag{2.19} $$

This implies that the primary gluon and all its descendants with $p \gg T$ will disappear via democratic branchings before having the time to lose a substantial fraction of their energy via drag. Hence, the dynamics of multiple branching is not significantly affected by the elastic collisions, so long as $p \gg T$.

However, the situation changes towards the late stages of the cascade when, as a result of successive branchings, the gluons have been degraded to lower energies $p \sim T$. Then, the various time-scales previously introduced become degenerate with each other (at least, parametrically),

$$ t_{\rm br}(T) \sim t_{\rm drag}(T) \sim t_{\rm rel} \sim \frac{1}{\bar{\alpha}^2 T \ln(1/\bar{\alpha})} \,, \tag{2.20} $$

meaning that the respective processes start to compete. Before having the time to branch again, the gluons with $p \sim T$ can approach a state of local thermal equilibrium, due to drag and diffusion. When this happens, the gluons from the jet cannot be distinguished anymore from the gluons in the plasma, hence the occupation numbers are typically of order one. This in particular implies that non-linear effects, like gluon recombination and the effects of the quantum statistics, cannot be ignored anymore. Due to the detailed balance principle — here, the balance between splittings and recombinations, — one expects the branching process to terminate in the approach to thermal equilibrium (see the discussion in section 3 below). Thus the in-medium cascade effectively ends at a scale $\sim T$.

From the previous discussion it should be clear that the characteristic time scale for the energy transfer from a relatively hard mini-jet ($p_0 \gg T$) to the medium is controlled by the branching dynamics and is of order $t_{\rm br}(p_0)$: this is the typical time after which the energy flows via democratic branchings from the primary gluon which has initiated the mini-jet to the soft gluons with $p \sim T$. The thermalization of the latter is a comparatively fast process, which takes a typical time $t_{\rm rel} \ll t_{\rm br}(p_0)$. The collisional time scale $t_{\rm drag}(p_0)$ — the would-be thermalization time for a gluon with the same initial energy in the absence of branchings — plays actually no role, since branchings are more efficient than elastic collisions in degrading the energy of the relatively hard ($p \gg T$) constituents of the jet.

3 The kinetic equation for the longitudinal dynamics

In this section we shall propose a kinetic equation which captures the general dynamics exposed in the previous section, to parametric accuracy at least, and which is simple enough to allow for explicit calculations, numerical and even semi-analytic.

The starting point is a kinetic equation introduced in ref. [36] and thoroughly derived in refs. [44] (see also refs. [27, 29] for an analysis of the quantum branching process, which justifies treating the successive branchings as independent from each other), with the schematic structure

$$\left(\frac{\partial}{\partial t} + \boldsymbol{v} \cdot \nabla_{\boldsymbol{x}} \right) f(t, \boldsymbol{x}, \boldsymbol{p}) \, = \, \mathcal{C}_{\rm el}[f] + \mathcal{C}_{\rm br}[f] \,. \tag{3.1}$$

Here, f is the gluon occupation number defined in eq. (2.7), which *a priori* refers to gluons from both the jet and the surrounding medium,[6] $\mathcal{C}_{\rm el}[f]$ is a collision integral encoding the $2 \rightarrow 2$ elastic collisions, whereas $\mathcal{C}_{\rm br}[f]$ encodes inelastic processes, like $2 \rightarrow 3$ or $1+(\text{many}) \rightarrow 2+(\text{many})$, which trigger nearly collinear branchings. In what follow, we shall denote the collinear splittings simply as $1 \rightarrow 2$. General expressions for the collision terms can be found in [44, 50]. A simpler form for $\mathcal{C}_{\rm br}[f]$, valid in the LPM regime, is presented in [36]. These collision terms are non-linear in f, as required by the detailed balance principle and the quantum statistics. Accordingly, the thermal Bose-Einstein distribution is a fixed point for both $\mathcal{C}_{\rm el}[f]$ and $\mathcal{C}_{\rm br}[f]$.

---

[6]To eq. (3.1), one should add corresponding equations for the quark and the antiquark occupation numbers, but here these are not necessary, since the (anti)quarks will only appear as constituents of the thermal medium.

The general equation (3.1) is however quite difficult to solve in practice, due to the non-linearity and also the non-locality of the collision integrals. Numerical solutions have been presented for special limits [39, 51, 52], which however do not cover the jet problem of interest for us here. In what follows, we shall therefore aim at simplifying this equation, in such a way to allow for qualitative but relatively straightforward studies. Similar approximations have been already used in the literature, separately for the elastic collisions and for the branching dynamics, but here we shall combine them for the first time in a study of the jet thermalization.

First, we would like to write an equation for the gluons from the jet *alone*. The surrounding medium will be merely treated as a thermal bath, which influences the jet dynamics but is not significantly disturbed by the latter. The omission of the back-reaction is indeed well justified, since the gluonic system produced by branchings remains dilute ($f(p) \ll 1$) down to the thermal scale $p \sim T$, as we have seen. This also means that the kinetic equation can be *linearized* w.r.t. the occupation number f for the gluons in the jet.

The distinction between the gluons in the jet and those in the medium is strictly possible for the energetic quanta with $p \gg T$, which control most stages of the branching process, but becomes ambiguous during the late stages, where all gluons have $p \lesssim T$. Notwithstanding, the discussion in the previous sections shows that the dynamics is rather smoothly changing around $p \sim T$, where the relevant time scales become commensurable with each other, cf. eq. (2.20). Hence, there should be no danger (to parametric accuracy, at least) with extrapolating down to $p \sim T$ an equation which is strictly valid for $p \gg T$. With that in mind, one can deduce rather simple approximations to the collision integrals in eq. (3.1).

Consider the elastic collisions first, which preserve the number of particles. Due to the infrared singularity of the Coulomb exchanges, the dominant contribution to the elastic collision integral comes from the small angle scatterings, i.e. from collisions with relatively small momentum transfer. This simplification strictly holds to leading logarithmic accuracy, since the momentum exchanges within the range $m_D \ll q \ll T$ produce a Coulomb logarithm $\ln(T^2/m_D^2) \sim \ln(1/\alpha_s)$ in the relevant transport coefficient (see below). Within this approximation, $\mathcal{C}_{\rm el}[f]$ can be replaced with the Fokker-Planck dynamics, which is physically equivalent to the Langevin dynamics introduced in section 2.2 [45–48]:

$$\mathcal{C}_{\rm el}[f] \simeq \frac{1}{4} \hat{q} \nabla_{\boldsymbol{p}} \cdot \left[\left(\nabla_{\boldsymbol{p}} + \frac{\boldsymbol{v}}{T} \right) f \right]. \tag{3.2}$$

In writing this expression, we have exploited the isotropy of the diffusion tensor and the Einstein relation between drag and diffusion, as already discussed in relation with eq. (2.14). It is easy to check that the above collision term admits the classical thermal distribution (the Maxwell-Boltzmann distribution for a massless particle) as a fixed point: $\mathcal{C}_{\rm el}[f_{\rm eq}] = 0$ for $f_{\rm eq}(\boldsymbol{p}) = \kappa \mathrm{e}^{-p/T}$, where κ is independent of $\boldsymbol{p}$, but otherwise arbitrary. For a dilute quark-gluon plasma (QGP) and to the leading logarithmic accuracy of interest, $\hat{q}$ is given by [46, 48, 49, 53]

$$\hat{q} = 8\pi \alpha_s^2 N_c \ln \left(\frac{\langle k_{\rm max}^2 \rangle}{m_D^2} \right) \int \frac{\mathrm{d}^3 \boldsymbol{p}}{(2\pi)^3} \left[N_c f_{\rm BE} (1 + f_{\rm BE}) + N_f f_{\rm FD} (1 - f_{\rm FD}) \right]$$

$$= \alpha_s N_c T m_D^2 \ln \left(\frac{\langle k_{\rm max}^2 \rangle}{m_D^2} \right), \tag{3.3}$$

where m_D is the leading-order result for the Debye screening mass, that is,

$$m_D^2 = \frac{2\pi}{3}\alpha_s T^2 \left(2N_c + N_f\right) , \qquad (3.4)$$

N_f is the number of active quark flavors, $\langle k_{\mathrm{max}}^2 \rangle \sim T^2$ is the maximal momentum transfer squared between the probe gluon and the medium constituents, and we have included contributions from both thermal gluons and thermal quarks, with respective occupation numbers

$$f_{\mathrm{BE}}(p) = \frac{1}{e^{\frac{p}{T}} - 1} , \qquad f_{\mathrm{FD}}(p) = \frac{1}{e^{\frac{p}{T}} + 1} . \qquad (3.5)$$

For the inelastic collision integral $\mathcal{C}_{\mathrm{br}}[f]$, one can use the corresponding approximation in ref. [36], which describes medium-induced gluon branching in the LPM regime, with the BDMPSZ branching rate shown in eq. (2.1). The original equation in [36] involves both splitting $(1 \to 2)$ and recombination $(2 \to 1)$ processes, but only the splitting terms survive after linearizing w.r.t. the gluon occupation number. The ensuing expression reads (see also refs. [27, 29])

$$\mathcal{C}_{\mathrm{br}}[f] \simeq \frac{1}{t_{\mathrm{br}}(p)} \int_0^1 \mathrm{d}x \, \mathcal{K}(x) \left[\frac{1}{x^{\frac{5}{2}}} f\left(t, \boldsymbol{x}, \frac{\boldsymbol{p}}{x}\right) - \frac{1}{2} f(t, \boldsymbol{x}, \boldsymbol{p}) \right] \qquad (3.6)$$

with $t_{\mathrm{br}}(p)$ as defined in eq. (2.5) and[7]

$$\mathcal{K}(x) \equiv \frac{[1 - x(1-x)]^{\frac{5}{2}}}{[x(1-x)]^{\frac{3}{2}}} . \qquad (3.7)$$

We recall that x and $1 - x$ represent the longitudinal momentum fractions of the daughter gluons. The two terms in the r.h.s. of eq. (3.6) are recognized as the gain and loss terms associated with a collinear splitting: in the gain term, a gluon with 3-momentum $\boldsymbol{p}$ is produced via the splitting of a parent gluon with momentum $\boldsymbol{p}/x$; in the loss term, a gluon with momentum $\boldsymbol{p}$ disappears because it splits. The integrand has singularities at $x = 0$ and $x = 1$, which however cancel between the gain and loss terms, and the integral is well defined. One can easily check that the branching integral (3.7) preserves the total energy: $\int \mathrm{d}^3\boldsymbol{p} \, |\boldsymbol{p}| \, \mathcal{C}_{\mathrm{br}}[f](\boldsymbol{p}) = 0$.

The collision integral in eq. (3.6) admits the turbulent spectrum $f \propto 1/p^{7/2}$ as a fixed point [28, 36, 41]. On the other hand, it does not vanish when f approaches the thermal distribution $f_{\mathrm{eq}}(\boldsymbol{p}) \propto \mathrm{e}^{-p/T}$. This is so because of the linearization, which is correct when $p \gg T$, but not also at softer momenta $p \sim T$, where the gluons from the jet can recombine with the gluons from the medium, thus effectively stopping the branching process in the approach to thermal equilibrium. An explicit treatment of such non-linear effects would

---

[7]Strictly speaking, the jet quenching parameter $\hat{q}$ which enters the expression (2.5) for the branching time is not exactly the same as that occurring in the Fokker-Planck term, eq. (3.2), because of the difference between the respective transverse scales $\langle k_{\mathrm{max}}^2 \rangle$: one has $\langle k_{\mathrm{max}}^2 \rangle \sim T^2$ for the Fokker-Planck dynamics and, roughly, $\langle k_{\mathrm{max}}^2 \rangle \sim \hat{q} t_{\mathrm{br}} \gg T^2$ for the branching of sufficiently energetic gluons (see the discussion in [54, 55]). Here however we shall ignore this subtle difference, which is anyway small, due to the weak, logarithmic, dependence upon $\langle k_{\mathrm{max}}^2 \rangle$, cf. eq. (3.3).

however greatly complicate the practical applications of our equation. To cope with that while keeping the formalism as simple as possible, we shall cut off by hand the branching process at some arbitrary scale $p_* \sim T$. In practice, we shall enforce the condition $p \geq p_*$ for all the particles participating in a $1 \rightarrow 2$ splitting process, that is, we shall require $p \geq p_*$ for the daughter gluons and hence $p \geq 2p_*$ for their parent. This cutoff p_* should be viewed as a free parameter of our model: the dependence of our predictions upon this scale, which as we shall see is weak so long as p_* remains of $\mathcal{O}(T)$, is indicative of the error that we have introduced by neglecting the non-linear terms in the (total) occupation number.

To summarize, our basic kinetic equation reads (with the compact notation $f_{\boldsymbol{p}} \equiv f(t, \boldsymbol{x}, \boldsymbol{p})$)

$$\left(\frac{\partial}{\partial t} + \boldsymbol{v} \cdot \nabla_{\boldsymbol{x}}\right) f_{\boldsymbol{p}} = \frac{1}{4}\hat{q}\,\nabla_{\boldsymbol{p}} \cdot \left[\left(\nabla_{\boldsymbol{p}} + \frac{\boldsymbol{v}}{T}\right) f_{\boldsymbol{p}}\right] + \frac{1}{t_{\mathrm{br}}(p)} \int_r \mathrm{d}x\, \mathcal{K}(x) \left[\frac{1}{x^{\frac{5}{2}}} f_{\frac{\boldsymbol{p}}{x}} - \frac{1}{2} f_{\boldsymbol{p}}\right], \quad (3.8)$$

where the symbol $\int_r$ denotes the restricted integration over x (see section 5 for details). This equation should be solved with the following initial condition at $t = 0$:

$$f(t = 0, \boldsymbol{x}, \boldsymbol{p}) = \frac{(2\pi)^3}{2(N_c^2 - 1)}\,\delta^{(3)}(\boldsymbol{x})\,\delta(p_z - E)\,\delta^{(2)}(\boldsymbol{p}_\perp)\,, \quad (3.9)$$

which represents the leading particle propagating along the z axis with energy $E \gg T$.

Eq. (3.8) matches our present purposes: it correctly encodes the dynamics of the relatively hard constituents of the jet with $p \gg T$ and, when extrapolated down to $p \lesssim T$, it also describes (at least to parametric accuracy) their approach to *kinetic* equilibrium — that is, the fact that the gluons from the jet individually approach a Maxwell-Boltzmann distribution in momentum, via elastic collisions in the plasma. On the other hand, the approach to *chemical* equilibrium — the evolution of the ensemble of the complete gluon distribution (jet+medium) towards the quantum Bose-Einstein distribution — is not encoded in this equation, but merely mimicked in a rather crude way by the lower cutoff p_* on the branching process.

Albeit considerably simpler than the original equations, eq. (3.8) is still too complicated to be solved as it stands, including via numerical techniques. A main source of complication is the spatial inhomogeneity inherent in our problem, which is very strong to start with, cf. eq. (3.9), and plays an essential role in the subsequent dynamics. In order to keep the salient features of this evolution in a numerically tractable way, we shall project eq. (3.8) along the longitudinal axis and at the same time perform approximations based on the separation of scales $p_z \gg p_\perp$ between longitudinal and transverse momenta. This separation is physically realized so long as $p \gg T$, which is the regime where eq. (3.8) strictly applies, but is progressively washed out when decreasing the momenta towards T. Yet, this approximation correctly keeps trace (to parametric accuracy, once again) of the separation of time scales in the problem: indeed, as already explained, the characteristic time scales for branching, eq. (2.5), and for the thermalization of hard particles, eq. (2.17), are controlled by the longitudinal momenta and become degenerate with each other (and with t_{rel}, eq. (2.16)) only when $p \sim T$.

Specifically, by integrating eq. (3.8) over the transverse phase-space, while at the same time approximating $p \simeq p_z$ within the definition of v_z, within $t_{\mathrm{br}}(p)$, and within the condition $p \geq p_*$, we finally obtain

$$
\left(\frac{\partial}{\partial t} + v_z \frac{\partial}{\partial z} \right) f_\ell(t, z, p_z) = \frac{1}{4} \hat{q} \frac{\partial}{\partial p_z} \left[\left(\frac{\partial}{\partial p_z} + \frac{v_z}{T} \right) f_\ell(t, z, p_z) \right]
$$
$$
+ \frac{1}{t_{\mathrm{br}}(p_z)} \int_r \mathrm{d}x \, \mathcal{K}(x) \left[\frac{1}{\sqrt{x}} f_\ell \left(t, z, \frac{p_z}{x} \right) - \frac{1}{2} f_\ell(t, z, p_z) \right] , \quad (3.10)
$$

where $v_z \equiv p_z / |p_z|$ and $f_\ell(t, z, p_z)$ is the longitudinal gluon distribution,[8]

$$
f_\ell(t, z, p_z) \equiv \frac{\mathrm{d}N_g}{\mathrm{d}z \mathrm{d}p_z} = \frac{2(N_c^2 - 1)}{(2\pi)^3} \int \mathrm{d}^2 \boldsymbol{x}_\perp \mathrm{d}^2 \boldsymbol{p}_\perp f(t, \boldsymbol{x}, \boldsymbol{p}) . \quad (3.11)
$$

In eq. (3.10) it is understood that the partial derivative $\partial_{p_z} \equiv \partial/\partial p_z$ commutes with v_z: $\partial_{p_z}(v_z f_\ell) = v_z \partial_{p_z} f_\ell$. (This prescription follows for the limit $p_\perp \ll p_z$: starting with $v_z = p_z/p$ with $p = \sqrt{p_z^2 + p_\perp^2}$, one obtains $\partial_{p_z} v_z = p_\perp^2/p^3 \simeq p_\perp^2/p_z^3$, which is much smaller than the respective natural value $\sim 1/p_z$.)

Eq. (3.10) is the equation that we shall explicitly study in what follows, via a combination of analytic and numerical methods.

4 Semi-analytic studies of the kinetic equation

As explained in the previous section, the two 'collision terms' in the r.h.s. of eq. (3.10) become important in different kinematical regions, which are complementary to each other: the high-energy region at $p \gg T$ for the branching term and, respectively, the low-energy region at $p \lesssim T$ for the elastic collisions. This distinction makes it possible to *separately* study their physical consequences — at least, at a qualitative level. Namely, one can effectively treat the branching process as a *source* of relatively soft gluons, which get injected into the medium at a scale $p_* \sim T$ and subsequently feel the effects of elastic collisions, in the form of drag and diffusion. These considerations motivate the following, simplified, version of the kinetic equation (3.10):

$$
\left(\frac{\partial}{\partial t} + v \frac{\partial}{\partial z} \right) f(t, z, p) = \frac{1}{4} \hat{q} \frac{\partial}{\partial p} \left[\left(\frac{\partial}{\partial p} + \frac{v}{T} \right) f(t, z, p) \right] + \mathcal{S}(t, z, p; p_*) . \quad (4.1)
$$

(From now on, we shall omit the subscript ℓ on f as well as the subscript z on longitudinal momenta and velocities, to simplify notations.) Notice that, when using this source approximation, we implicitly assume that the medium acts as a perfect sink: the branching dynamics at $p > p_*$ is not at all affected by collisions. For consistency, one must also construct the source $\mathcal{S}(t, z, p)$ by assuming an 'ideal' gluon cascade, with wave turbulence, at $p > p_*$. This source has the general structure

$$
\mathcal{S}(t, z, p; p_*) = \delta(t - z)\delta(p - p_*)\,\Gamma(t, p_*) , \quad (4.2)
$$

---

[8]Notice that this quantity f_ℓ is not an occupation number by itself (because of the integration over the transverse phase-space in eq. (3.11)), so in practice one can very well have $f_\ell > 1$ and still use a linear kinetic equation, provided one can justify that the actual occupation number is indeed small.

where $\Gamma(t, p_*)$ is the flux of gluons at the lower end of the cascade at time t. This flux can be easily inferred from the previous studies of the 'ideal' branching process [28, 30] and will be presented in section 4.2.2 below. Our ultimate purpose in this section is to solve eq. (4.1) with this particular source.

In preparation to that, it will be useful to study a simpler case, that of a steady source which propagates at the speed of light. Then, in section 4.2.1, we shall construct the exact Green's function for the differential operator appearing in eq. (4.1). Finally, in section 4.2.2, we shall use this Green's function to give a semi-analytic calculation of the gluon distribution produced by the physical source.

4.1 Thermalization for a steady source

In this subsection we shall present an exact solution for the case where the time-dependence of the injection rate $\Gamma(t, p_*)$ in the r.h.s. of eq. (4.2) can be neglected. This is a good approximation if one is interested in the effects of the collisions over a time interval Δt which is much smaller than the characteristic time scale $t_{\mathrm{br}}(E)$ for the evolution of the source via branchings, but much larger than t_{rel} (in order for the effects of collisions to be indeed significant); that is, $t_{\mathrm{rel}} < \Delta t \ll t_{\mathrm{br}}(E)$. During this time Δt, the source can be effectively treated as 'frozen' and the corresponding distribution at $z \leq t$ is expected to depend only on $t - z$.

For convenience, we choose to normalize the injection rate as $\Gamma(t, p_*) = T$. (This brings no loss of generality since the equation is linear.) Also, within the context of this subsection, it is preferable to denote the energy of the soft gluons as p_0, rather than p_*. With these conventions, eq. (4.1) becomes (below, a prime denotes a derivative w.r.t. $\hat{p}$)

$$\left(\frac{\partial}{\partial \hat{t}} + v\frac{\partial}{\partial \hat{z}}\right) f = (f' + vf)' + \delta(\hat{t} - \hat{z})\delta(\hat{p} - \hat{p}_0), \tag{4.3}$$

in terms of dimensionless variables which measure the respective quantities in natural units, that is, in units of t_{rel} for all the time and length scales ($\hat{t} = t/t_{\mathrm{rel}}$, $\hat{z} = z/t_{\mathrm{rel}}$) and in units of T for the various momenta ($\hat{p} = p/T$, etc). In what follows, we shall use such reduced variables in most formulæ, to simplify the notation, but we shall restore the physical units when discussing the physical interpretation of the results. Also, we shall drop the hat on the reduced variables (e.g. $\hat{p} \to p$), as the distinction should be clear from the context.

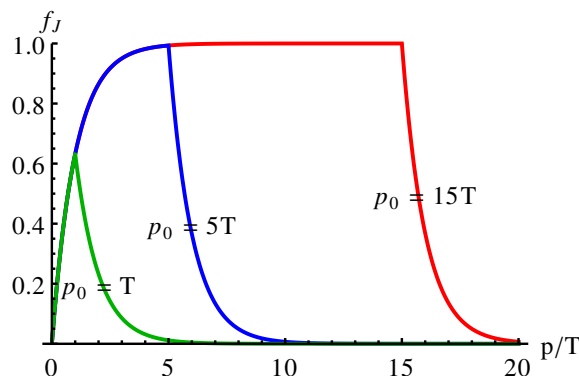We search for a stationary distribution $f(x^-, p; p_0)$ with $x^- \equiv t - z$. This function obeys

$$\begin{cases} 0 = (f' + f)' + \delta(x^-)\delta(p - p_0) & \text{for } p > 0, \\ 2\dfrac{\partial}{\partial x^-} f = (f' - f)' & \text{for } p < 0. \end{cases} \tag{4.4}$$

together with the condition for particle number conservation at $p = 0$:

$$\left(f' + f\right)\big|_{p=0^+} = \left(f' - f\right)\big|_{p=0^-} = \delta(x^-). \tag{4.5}$$

For $p > 0$ the solution to eq. (4.4) is found in the form

$$f(x^-, p; p_0) = f_{\mathrm{J}}(p, p_0)\delta(x^-) + C^+(x^-)\,\mathrm{e}^{-p} \tag{4.6}$$

Figure 2. The jet front function $f_{\mathrm{J}}(p, p_0)$ is displayed as a function of p for $p_0/T = 1, 5$ and 15.

where $f_{\mathrm{J}}(p, p_0)$ is the 'jet front function' (see also figure 2)

$$f_{\mathrm{J}}(p, p_0) \equiv \mathrm{e}^{-p} \left(\mathrm{e}^{p_0} - 1 \right) \theta(p - p_0) + \left(1 - \mathrm{e}^{-p} \right) \theta(p_0 - p) \,, \tag{4.7}$$

and $C^+(x^-)$ is an unknown function, to be later determined. For $p < 0$, it is convenient to use the Laplace transform of the solution, $f_s(p) \equiv \int_0^\infty \mathrm{d}x^- \mathrm{e}^{-sx^-} f(x^-, p; p_0)$. By taking the Laplace transform in the second equation (4.4), one obtains

$$f_s(p) = \tilde{C}^-(s) \mathrm{e}^{\frac{p}{2}(\sqrt{1+8s}+1)} \qquad \text{for } p < 0 \,. \tag{4.8}$$

By imposing the conservation condition (4.5) (which actually introduce two constraints), we can determine both 'coefficient' functions $\tilde{C}^-(s)$ and $\tilde{C}^+(s)$ (the Laplace transform of $C^+(x^-)$):

$$\tilde{C}^+(s) = \tilde{C}^-(s) = \frac{2}{\sqrt{8s+1}-1} \,. \tag{4.9}$$

After also performing the inverse Laplace transformation, we finally obtain

$$f(t-z, p; p_0) = \begin{cases} f_{\mathrm{J}}(p, p_0)\delta(t - z) + \left[\frac{1}{4}\mathrm{erf}\left(\frac{\sqrt{t-z}}{2\sqrt{2}} \right) + \frac{1}{4} + \frac{\mathrm{e}^{-\frac{t-z}{8}}}{\sqrt{2\pi}\sqrt{t-z}} \right] \mathrm{e}^{-p} & \text{for } p \geq 0, \\ \frac{1}{4}\mathrm{e}^p \left[\mathrm{erf}\left(\frac{2p+t-z}{2\sqrt{2}\sqrt{t-z}} \right) + 1 \right] + \frac{\mathrm{e}^{-\frac{(-2p+t-z)^2}{8(t-z)}}}{\sqrt{2\pi}\sqrt{t-z}} & \text{for } p \leq 0. \end{cases} \tag{4.10}$$

We have introduced here the error function

$$\mathrm{erf}(x) \equiv \frac{2}{\sqrt{\pi}} \int_0^x \mathrm{d}t \, \mathrm{e}^{-t^2} \,. \tag{4.11}$$

By inspection of the solution in eq. (4.10), one can recognize a *front* which propagates at the speed of light with the profile in p shown in figure 2, and a *tail* at $z < t$ which is localized around $p = 0$. The overall distribution is illustrated in figure 3 for the case $p_0 = T$, which is the most interesting one for the physical problem at hand (recall that $p_0 \equiv p_*$ is the infrared end of the gluon cascade). However, in order to better appreciate the physical content of this stationary distribution, it is useful to consider first the high-energy case $p_0 \gg T$. Then, as visible in figure 2, the front profile becomes a θ-function with support
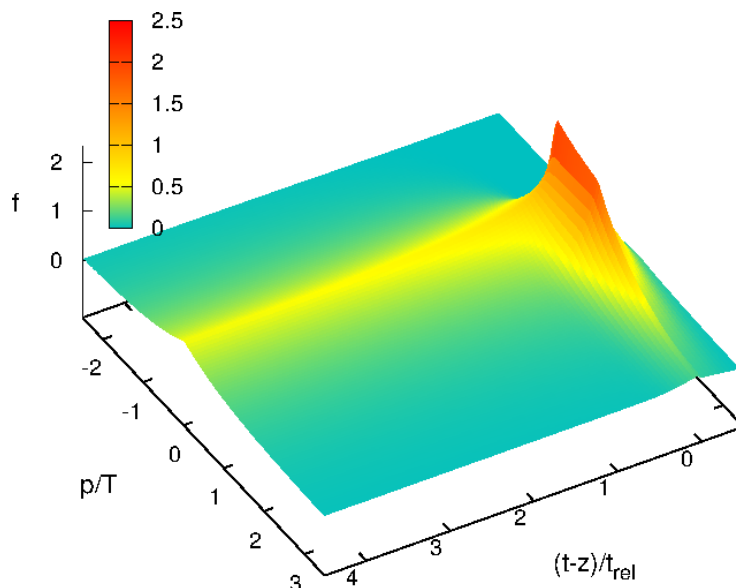
Figure 3. The distribution (4.10) as produced by a steady source is shown as a function of $t - z$ and p for $p_0 = T$. This figure exhibits a front moving along the light-cone at $z = t$ and a thermalized tail at $z \lesssim t - t_{\rm rel}$. In displaying the front, the δ-function in eq. (4.10) is regulated as $\delta_\epsilon(t - z) = \frac{1}{\sqrt{\epsilon\pi}}{\rm e}^{-\frac{(t-z)^2}{\epsilon}}$ with $\epsilon = 0.1$.

at $0 < p < p_0$. This can be understood as follows: a particle injected by the source at time t_0 with $p_0 \gg T$ loses energy towards the medium at a constant rate, via drag (recall the discussion following eq. (2.14)); hence, its energy decreases with time according to

$$p(t) = p_0 - (T/t_{\rm rel})(t - t_0). \tag{4.12}$$

So long as this energy remains much larger than T, which is indeed the case during a large interval $t - t_0 \simeq (p_0/T)t_{\rm rel} \gg t_{\rm rel}$, the diffusion effects are negligible and the distribution created by this particle can be as well studied by neglecting the second-order derivative f'' in eq. (4.3). The corresponding solution is easily found as

$$f(t - z, p; p_0) = \delta(t - z)\theta(p_0 - p)\theta(p) \qquad \text{(without diffusion)}, \tag{4.13}$$

which is indeed very similar to the 'front' piece of eq. (4.10) in the case $p_0 \gg T$. Hence, the 'front' is built with those particles that have been recently injected by the source, within a time interval $\Delta t = (p_0/T)t_{\rm rel}$ prior to the time t of measurement, and which have a still a relatively large energy $p \gtrsim T$ at time t. All the other particles, that have been injected at earlier times $t' < t - (p_0/T)t_{\rm rel}$, have been degraded by the viscous drag to energies $p \lesssim T$, where the diffusion effects *are* important. This becomes clear by inspection of the function $f_{\rm J}(p, p_0)$ for $p_0 = 1$ in figure 2.

As a consequence of the competition between diffusion and drag, the gluons with $|p| \lesssim T$ can have both positive and negative velocities, hence their distribution moves at a slower speed $|v| < 1$ This explains the depletion visible in f_J at $p \lesssim T$ (for any p_0) and also the formation of the tail. At points sufficiently far away from the front, such that

$t - z \gg t_{\rm rel}$, the distribution reaches thermal equilibrium, since this is the fixed point of the Fokker-Plank dynamics. Indeed, the solution in eq. (4.10) implies

$$f(t - z, p; p_0) \simeq \frac{1}{2} \, \mathrm{e}^{-|p|/T} \quad \text{when} \ \ t - z \gg t_{\rm rel} \,. \tag{4.14}$$

To understand the energy balance between the jet and the medium, notice that the external source in eq. (4.3) inserts energy at a rate $\mathrm{d}E_s/\mathrm{d}t = p_0 T$, whereas the energy carried by the thermalized tail $t - z \gg t_{\rm rel}$ increases at a rate $\mathrm{d}E_{\rm ther}/\mathrm{d}t = T^2$. (The total energy carried by the front is independent of time, $E_{\rm J} = \int \mathrm{d}p p f_{\rm J}(p, p_0) \sim t_{\rm rel} p_0^2$, and represents only a negligible fraction of the total energy injected by the source over large times.) If $p_0 \gg T$, then the insertion rate is much larger than the thermalization rate, meaning most of the energy is lost via viscous drag — that is, it is transferred via collisions to the medium constituents. By choosing $p_0 \simeq T$, i.e. by inserting the particles directly at the medium scale, we can minimize the effects of the drag and thus recover most of the injected energy in the thermalized tail.

The qualitative features that we have discovered in this simple example are in fact generic and will be recovered in the more general situations to be studied later on. In particular, the peculiar structure of the distribution visible in figure 3, with a jet localized on the light-cone ($z = t$) and a thermalized tail well behind it ($z < t - t_{\rm rel}$), will also show up for a physical jet initiated by a leading particle with energy $E \gg T$, at least for sufficiently small times $t \lesssim t_{\rm br}(E)$.

4.2 Jet quenching in the source approximation

In this subsection we shall use the source approximation, cf. eq. (4.1), in order to unveil generic features of the jet evolution in the presence of both branchings and elastic collisions. The solution to eq. (4.1) corresponding to a general source $\mathcal{S}(t, z, p)$ can be written as

$$f(t, z, p) = \int \mathrm{d}p_0 \mathrm{d}z_0 \, f_G(t, z - z_0, p, p_0) f_0(z_0, p_0)$$
$$+ \int \mathrm{d}p_0 \mathrm{d}z_0 \int_{-\infty}^{t} \mathrm{d}t' f_G(t - t', z - z_0, p; p_0) \mathcal{S}(t', z_0, p_0), \tag{4.15}$$

where we have chosen the initial condition $f(0, z, p) = f_0(z, p)$ and f_G is the appropriate Green's function, that is, the solution to the homogeneous equation

$$\left(\frac{\partial}{\partial t} + v \frac{\partial}{\partial z} \right) f_G(t, z, p) = \frac{\partial}{\partial p} \left[\left(\frac{\partial}{\partial p} + v \right) f_G(t, z, p) \right], \tag{4.16}$$

with initial condition $f_G(0, z, p; p_0) = \delta(z) \delta(p - p_0)$ with $p_0 > 0$. An analytic form for this Green's function will be constructed in the next subsection and then applied to the source representing an ideal branching process, in section 4.2.2.

4.2.1 The Fokker-Planck Green's function

The Green's function for the longitudinal Fokker-Planck equation can be constructed via a mathematical method similar to that described in the previous subsection for the case of

a steady source. In what follows, we shall omit the details but merely show the starting point equations, which replace the previous equations (4.4) and (4.5). After performing Laplace and Fourier transforms with respect to t and z respectively, we deduce

$$\begin{cases} (s + iQ) - \delta(p - p_0) = f''_{sQ} + f'_{sQ} & \text{for } p > 0, \\ s f_{sQ} - iQ f_{sQ} = f''_{sQ} - f'_{sQ} & \text{for } p < 0, \end{cases} \tag{4.17}$$

together with the following condition for the number conservation

$$\left(f'_{sQ} + f_{sQ} \right)\big|_{p=0^+} = \left(f'_{sQ} - f_{sQ} \right)\big|_{p=0^-}, \tag{4.18}$$

where f_{sQ} is a compact notation for a function of two arguments, s and Q, defined as

$$f_{sQ} \equiv \int_0^\infty dt\, e^{-st} \int dz\, e^{-iQz} f(t, z, p). \tag{4.19}$$

After lengthy but straightforward mathematical manipulations, one finally obtains

$$f_G(t, z, p; p_0) = \theta(p) f_G^+(t, z, p; p_0) + \theta(-p) f_G^-(t, z, p; p_0), \tag{4.20}$$

where (with $t \geq |z|$)

$$f_G^+(t, z, p; p_0) = \frac{e^{-\frac{p_0 - p}{2} - \frac{t}{4}}}{2\sqrt{\pi t}} \left[e^{-\frac{(p - p_0)^2}{4t}} - e^{-\frac{(p + p_0)^2}{4t}} \right] \delta(t - z)$$

$$+ \frac{e^{-\frac{(p + p_0 - z)^2}{4t} - p}}{8\sqrt{\pi} t^{5/2}} \left[t(t + 2) - (p + p_0 - z)^2 \right] \text{erfc}\left(\frac{1}{2}\sqrt{t - \frac{z^2}{t}}\left(\frac{p + p_0}{t + z} - 1 \right) \right)$$

$$+ \frac{(t + z)(p + p_0 + t - z)}{4\pi t^2 \sqrt{t^2 - z^2}} e^{-\frac{(p + p_0)^2}{2(t + z)} + \frac{p_0 - p}{2} - \frac{t}{4}}, \tag{4.21}$$

and

$$f_G^-(t, z, p; p_0) = \frac{(t + z)(p_0 + t - z) - p(t - z)}{4\pi t^2 \sqrt{t^2 - z^2}} e^{-\frac{p^2}{2(t - z)} + \frac{p + p_0}{2} - \frac{p_0^2}{2(t + z)} - \frac{t}{4}} \tag{4.22}$$

$$+ \frac{e^{p - \frac{(p + p_0 - z)^2}{4t}}}{8\sqrt{\pi} t^{5/2}} \left[t(t + 2) - (p + p_0 - z)^2 \right] \text{erfc}\left(\frac{1}{2}\sqrt{t - \frac{z^2}{t}}\left(\frac{p_0}{t + z} - \frac{p}{t - z} - 1 \right) \right).$$

In these formulæ, we have introduced the complementary error function $\text{erfc}(x) \equiv 1 - \text{erf}(x)$ (cf. eq. (4.11)). Also, we have used reduced variables $p \to p/T$, $t \to t/t_{\text{rel}}$ etc., to simplify writing (recall the discussion after eq. (4.3)). The above expression for f_G is normalized to unity w.r.t. these reduced variables: $\int dz dp\, f_G(t, z, p; p_0) = 1$. In order to obtain the properly normalized Green's function in physical units, one must divide the result in eqs. (4.21)–(4.22) by the dimensionless product $T t_{\text{rel}}$ and replace all the reduced variables by their physical counterparts ($p \to p/T$, etc).
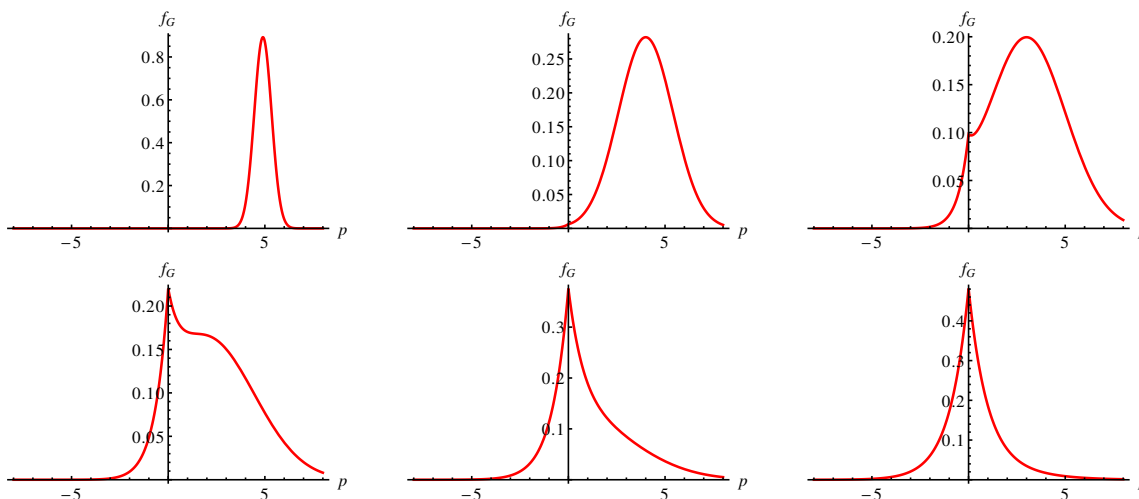
Figure 4. The 'reduced' Green's function in eq. (4.23) plotted as a function of p for $p_0 = 5$ and 6 successive values of time: $t = 0.1, 1, 2, 3, 5, 10$.

The above expression for f_G looks quite involved. In order to unveil its physical content, it is useful to first consider its simpler version obtained after integrating over z:

$$f_G(t,p;p_0) = \begin{cases} \dfrac{1}{4}\,\mathrm{e}^{-p}\,\mathrm{erfc}\Big(\dfrac{p+p_0-t}{2\sqrt{t}}\Big) + \dfrac{1}{2\sqrt{\pi t}}\,\mathrm{e}^{-\frac{(p-p_0+t)^2}{4t}} & \text{for } p > 0 \\[3mm] \dfrac{1}{4}\,\mathrm{e}^{p}\,\mathrm{erfc}\Big(\dfrac{-p+p_0-t}{2\sqrt{t}}\Big) + \dfrac{\mathrm{e}^{p}}{2\sqrt{\pi t}}\,\mathrm{e}^{-\frac{(-p+p_0-t)^2}{4t}} & \text{for } p < 0. \end{cases} \tag{4.23}$$

This function describes the relaxation of an initial perturbation which is homogeneous in z but localized in momentum: $f_G(0,p;p_0) = \delta(p - p_0)$. (See figure 4 for a graphical illustration.) For $p_0 \gg T$ and sufficiently small times, such that $\frac{t}{t_{\rm rel}} \ll \frac{p_0}{T}$, $f_G(t,p;p_0)$ is dominated by its Gaussian component at $p > 0$, that is,

$$f_G(t,p;p_0) \simeq \frac{1}{2\sqrt{\pi t}}\,\mathrm{e}^{-\frac{(p-p_0+t)^2}{4t}} \qquad \text{when } t \ll p_0\,. \tag{4.24}$$

This describes the damping of the original energy via drag and also the broadening of the longitudinal momentum distribution due to diffusion, in agreement with the discussion in section 2.2:

$$\langle p(t)\rangle \simeq p_0 - (T/t_{\rm rel})t\,, \qquad \langle p^2\rangle - \langle p\rangle^2 \simeq 2\hat{q}t\,. \tag{4.25}$$

But already for such small values of time, there is a second component (represented by the two terms proportional to the complementary error function) which starts growing around $p = 0$. This corresponds to particles which have essentially lost their original energy and pile up around $p = 0$, via diffusion. For larger times $t \gtrsim (p_0/T)t_{\rm rel}$, this component becomes the dominant one and rapidly approaches the thermal distribution (notice that $\mathrm{erfc}(x) \to 2$ when $x \to -\infty$):

$$f_G(t,p;p_0) \simeq \frac{1}{2}\,\mathrm{e}^{-|p|} \qquad \text{when } t \gg p_0\,. \tag{4.26}$$
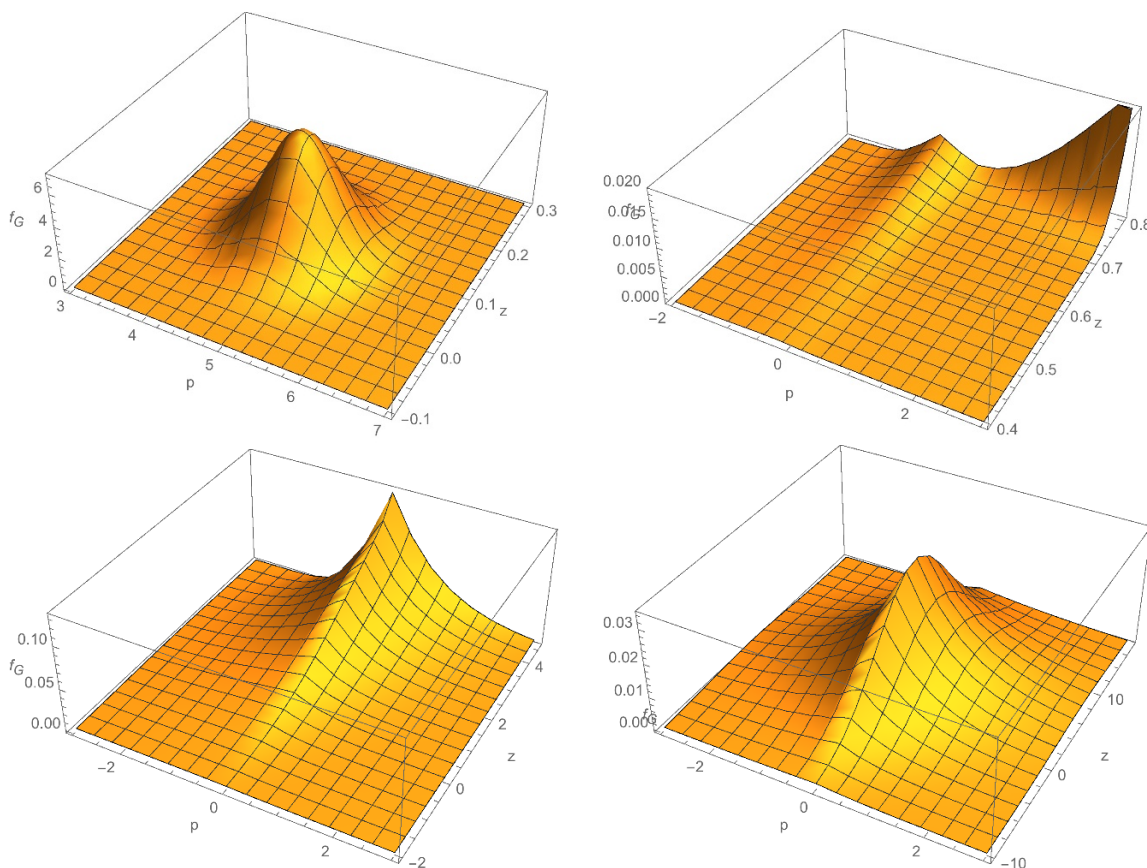
Figure 5. The Green's function in eqs. (4.21)–(4.22) plotted as a function of p and z for $p_0 = 5$ and four values of t: upper line, left: $t = 0.1$; upper line, right: $t = 1$; lower line, left: $t = 5$; lower line, right: $t = 20$. Note that the vertical scales and also the ranges in p and z can significantly differ from one figure to another. For $t \gtrsim 1$, one can see the emergence and growth of a thermal tail at $|z| \ll t$, which for $t \gg p_0$ is the Gaussian shown in eq. (4.27).

Turning now to the general case with z-dependence, eqs. (4.21)–(4.22) show that, at early times, $t \ll (p_0/T)t_{\rm rel}$, there is a remnant of the original perturbation — the 'jet front' localized at $z = t$, as described by the first term in the r.h.s. of eq. (4.21) — whose momentum distribution is however degrading with time, in the same way as in eq. (4.24) (see also figure 5). With increasing time, this 'jet front' is gradually washed out and a new distribution develops around $p = 0$, which is slowly varying in z (for $|z| \ll t$ at least). For sufficiently large times, $t \gg (p_0/T)t_{\rm rel}$, and sufficiently far behind the front, $z \lesssim t - t_{\rm rel}$, this new distribution is thermal in p, hence it describes local thermal equilibrium:

$$f_G(t, z, p; p_0) \simeq \frac{{\rm e}^{-|p|}}{2} \, \frac{{\rm e}^{-\frac{(z-p_0)^2}{4t}}}{2\sqrt{\pi t}} \quad \text{when } t \gg p_0 \gg 1 \text{ and } |z| \ll t. \qquad (4.27)$$

This is recognized as the product between the Maxwell-Boltzmann distribution in momentum, cf. eq. (4.26), and the one-dimensional heat kernel describing diffusion in z. Eq. (4.27) shows that the large-time distribution is centered around $z = (p_0/T)t_{\rm rel}$ (the maximal distance travelled by the original perturbation until it has lost all its energy, due to drag)

– 23 –

and that its longitudinal extent grows with time, according to $\Delta z(t) \simeq \sqrt{4 t_{\mathrm{rel}} t}$. Thus, remarkably, the momentum-space diffusion originally encoded in the Fokker-Planck equation has also generated *spatial* diffusion. One may chose as a criterion for having a quasi-homogeneous distribution the condition that the longitudinal extent $\Delta z(t)$ be larger than the location $(p_0/T) t_{\mathrm{rel}}$ of the center. This happens for

$$t \gtrsim \frac{1}{4} \left(\frac{p_0}{T} \right)^2 t_{\mathrm{rel}} , \tag{4.28}$$

a time scale considerably larger than that required by the thermalization of the momentum distribution. Note finally that by integrating eq. (4.27) over z and over p we recover, to the accuracy of interest, the normalization of the initial perturbation, i.e. $\int \mathrm{d}z \mathrm{d}p \, f_G(t, z, p) = 1$, which confirms that the whole perturbation has thermalized. If on the other hand one computes the total energy contained in the thermalized distribution (4.27) one finds, clearly, $\int \mathrm{d}z \mathrm{d}p \, |p| \, f_G(t, z, p) \simeq T$ for $t \gg (p_0/T) t_{\mathrm{rel}}$. That is, out of the total energy $p_0 > T$ of the original perturbation, a fraction T/p_0 is carried at large times by the thermalized distribution, whereas the remaining fraction $(p_0 - T)/p_0$ has been transmitted to the medium, via drag. This conclusion on the energy loss is similar to our previous findings for the case of a stationary source in section 4.1.

4.2.2 A physical source generated by the branching process

In this subsection we apply the Green's function method to the main physical problem of interest, namely a source generated by a branching process. More precisely, we consider an *ideal* branching process, for which the splitting dynamics at $p > p_*$ is not at all influenced by elastic collisions: the medium solely acts as a 'perfect sink' which absorbs the energy of the gluon cascade at the 'infrared' scale $p_* \sim T$. (A more general situation will be studied in section 5.) Under these circumstances, the source has the structure shown in eq. (4.2) with $\Gamma(t, p_*) = \mathcal{F}(E, p_*, t)/p_*$. Here, $\mathcal{F}(E, p_*, t)$ is the energy flux at p_* generated at time t by a cascade that was initiated at $t = 0$ by a leading particle with initial energy $E \gg T$ (recall the discussion in section 2.1). This source truly represents a bunch of relatively soft particles, which carry all the same energy p_*, move together at the speed of light, and whose number is evolving in time due to the branching dynamics.

Within the context of the ideal cascade, one was able to obtain an exact analytic result for this function $\mathcal{F}(E, p_*, t)$ [28]. Strictly speaking, the analysis in [28] required two additional assumptions, which are not essential from the viewpoint of physics, but simplify the mathematical manipulations:

(a) the energy E of the LP is not *too* large, namely it obeys[9] $E \leq \omega_c(L) \equiv \hat{q} L^2$, where the upper limit $\omega_c(L) = \omega_{\mathrm{br}}(L)/\bar{\alpha}^2$ is parametrically larger than $\omega_{\mathrm{br}}(L)$ at weak coupling;

(b) the kernel (3.7) within the BDMPSZ splitting rate is replaced by its simplified version $\mathcal{K}_0(x) \equiv 1/[x(1-x)]^{\frac{3}{2}}$, which preserves the correct behavior near the singular endpoints at $x = 0$ and $x = 1$.

---

[9]The generalization of the subsequent results to more energetic jets with $E \gg \omega_c(L)$ can be found in ref. [30].

Under these assumptions, the energy flux is obtained as [28]

$$\mathcal{F}(E, p_*, t) = 2\pi E \frac{t}{t_{\rm br}^2(E)}\, {\rm e}^{-\pi t^2/t_{\rm br}^2(E)} \;=\; \frac{\rm d}{{\rm d}t}\, \Delta E_{\rm flow}\,, \tag{4.29}$$

where $t_{\rm br}(E)$ is the branching time introduced in eq. (2.5) (the typical time after which a parton with energy E undergoes the first democratic branching) and

$$\Delta E_{\rm flow}(E, p_*, t) = E\left[1 - {\rm e}^{-\pi t^2/t_{\rm br}^2(E)}\right] = E\left[1 - {\rm e}^{-\pi \omega_{\rm br}(t)/E}\right] \tag{4.30}$$

with $\omega_{\rm br}(t) = \bar{\alpha}^2 \hat{q} t^2$, is the energy which accumulates into the soft modes with $p \leq p_*$ after a time t. The above results strictly apply for $p_* \ll \omega_{\rm br}(t)$, or, equivalently $t \gg t_{\rm br}(p_*) \sim t_{\rm rel}$, and within that regime they are independent of p_*. In fact, in the absence of the sink at p_*, this whole energy would accumulate in a condensate at $p = 0$ [28].

Eq. (4.30) confirms that the time scale $t_{\rm br}(E)$ plays the role of the lifetime of the leading particle w.r.t. democratic branchings. At small times $t \ll t_{\rm br}(E)$, one can expand the exponential there to lowest order and thus find

$$\Delta E_{\rm flow}(t) \simeq \pi \omega_{\rm br}(t) \quad \text{when} \quad t \ll t_{\rm br}(E)\,. \tag{4.31}$$

Alternatively, this estimate is correct for a given time t provided the energy E of the LP is sufficiently high, $E \gg \omega_{\rm br}(t)$. This result is in agreement with (2.6) up the replacement $\upsilon \to 2\pi$, due to the use of the approximate kernel $\mathcal{K}_0(x)$. It shows that, at small times, the energy loss via flow is independent of E (essentially, because the LP does not 'feel' the change in its own energy due to flow) and that it grows with time like t^2. As explained in section 2, this 'small time' (or 'high energy') regime is the most interesting one for jets at the LHC, where one indeed has $E \gg \omega_{\rm br}(L)$, with L the size of the medium.

For larger times, such that $t \sim t_{\rm br}(E)$ or, equivalently, $E \sim \omega_{\rm br}(t)$, the LP disappears via democratic branching and its whole initial energy is carried away by the flow. This is indeed consistent with eq. (4.31) which shows that $\Delta E_{\rm flow}(t) \simeq E$ when $t \gtrsim t_{\rm br}(E)$. From a physical viewpoint, this 'large time' (or 'low energy') regime better corresponds to the primary gluons radiated by the LP, which evolve into 'mini-jets'.

It is also interesting to notice the time dependence of the energy flux in eq. (4.29): this rises linearly with t at small times, then reaches a maximal value around $t = t_{\rm br}(E)$, and rapidly vanishes at larger times. This means that the production rate for soft gluons is largest towards the late stages of the branching process, i.e. for $t \sim t_{\rm br}(E)$, just before the LP dies away.

We now return to the solution to the Fokker-Planck equation for the physical source at hand. Using eq. (4.2), the integrals over z_0 and p_* in eq. (4.15) can be immediately performed to yield

$$f(t, z, p) = \frac{1}{p_*} \int_0^t {\rm d}t'\, f_G(t - t', z - t', p; p_*)\, \mathcal{F}(t')\,. \tag{4.32}$$
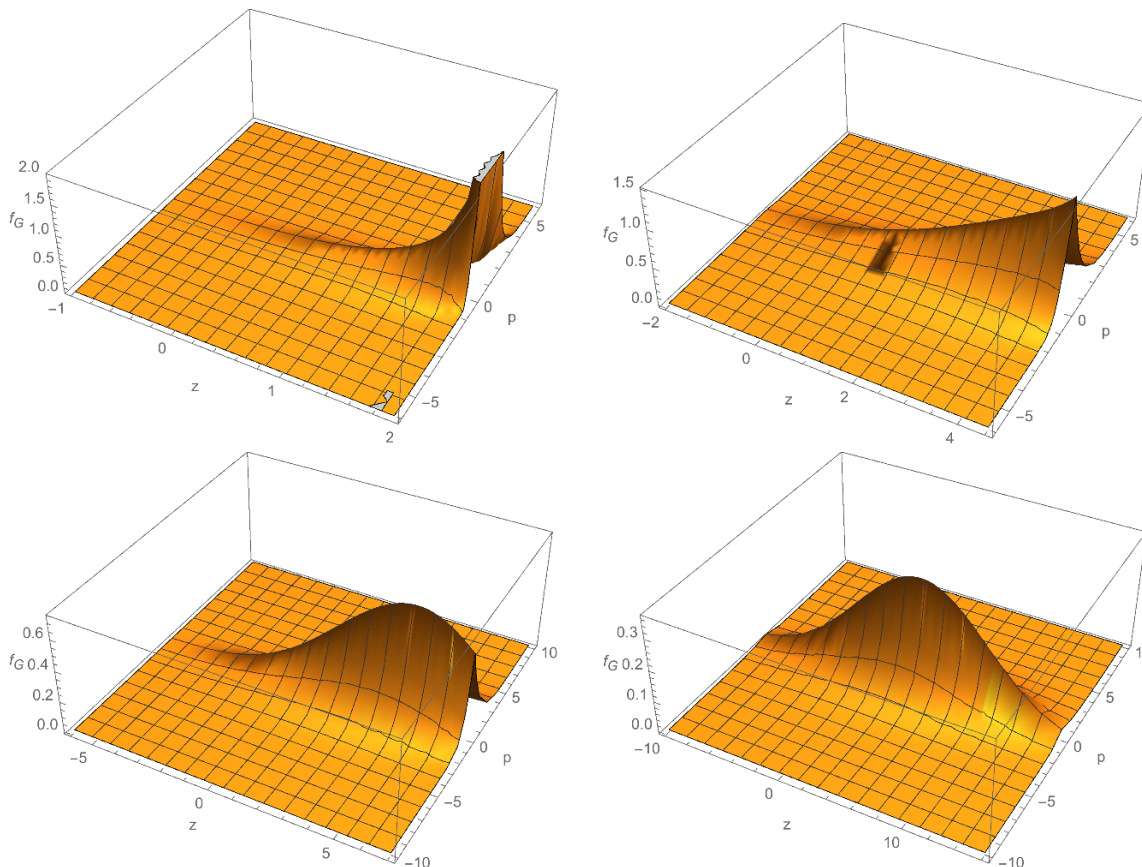
Figure 6. The distribution (4.32) produced by the source in eq. (4.29) with $t_{\mathrm{br}}(E) = 6$ and $p_* = 1$ is plotted as a function of p and z for four values of t: upper line, left: $t = 2$; upper line, right: $t = 5$; lower line, left: $t = 8$; lower line, right: $t = 20$. For relatively small times $t < t_{\mathrm{br}}(E)$, the source is still active and the distribution is thermal only in the tail at $z < t - t_{\mathrm{rel}}$. For larger times $t > t_{\mathrm{br}}(E) + p_*$, the source has essentially decayed and the distribution is thermal at any z. For $t = 20$ there is no significant difference between the exact result displayed above and the respective prediction of the diffusion approximation (4.33).

It seems difficult to analytically perform the remaining integral over t', but this can be numerically computed, with the results shown in figure 6 (in terms of reduced variables).[10] These results can be understood as follows: for relatively small times, $t \ll t_{\mathrm{br}}(E)$, the source (the leading particle) is still present and the gluon distribution is quite similar to that produced by a stationary source, as shown in figure 3: it exhibits a front at $z = t$ and $0 < p < p_*$ (but with the edges smeared out by diffusion), which represents the gluons that have been recently emitted, and with a tail at $z < t$ and peaked in momentum at $p = 0$, which describes the gluons which have experienced the effects of collisions. For later times $t \gtrsim t_{\mathrm{br}}(E)$, the source has disappeared via democratic branching and the

---

[10]When rewriting eq. (4.1) in terms of reduced variables, we find that the dimensionless version of the source in eq. (4.2) reads (we restore the hat on reduced quantities, for more clarity): $\hat{\mathcal{S}} = \theta(\hat{t})\delta(\hat{t} - \hat{z})\delta(\hat{p} - \hat{p}_*)(\hat{\mathcal{F}}/\hat{p}_*)$, where $\hat{\mathcal{F}} \equiv \mathcal{F}/T^2 = 8\pi\bar{\alpha}^2\hat{t}\exp\{-\pi\hat{t}^2/\hat{t}_{\mathrm{br}}^2(E)\}$ depends upon the energy E only via the reduced branching time $\hat{t}_{\mathrm{br}}(E) \equiv t_{\mathrm{br}}(E)/t_{\mathrm{rel}}$.

gluon distribution looks quite similar to that produced by a localized source at late times, cf. figure 5: a thermal distribution in momentum which extends in z via diffusion and which peaks around $z = t_{\rm br}(E)$ (the maximal displacement of the source before it dies away).

In fact, for sufficiently large time, $t - t_{\rm br}(E) \gg (p_*/T)t_{\rm rel} \sim t_{\rm rel}$, one can use the diffusion approximation for the Green's function, eq. (4.27), to deduce (in reduced variables, cf. footnote 10)

$$f(t, z, p) \simeq 4\pi\bar{\alpha}^2 \, \frac{{\rm e}^{-|p|}}{p_*} \int_0^t {\rm d}t' \, t' \, \frac{{\rm e}^{-\frac{(z-t')^2}{4(t-t')}}}{\sqrt{4\pi(t-t')}} \, {\rm e}^{-\pi t'^2/t_{\rm br}^2(E)} \,. \tag{4.33}$$

This represents the medium perturbation that would be left over by a relatively soft mini-jet ($E \ll \omega_{\rm br}(t)$), after it thermalizes. By integrating this late-time distribution over z and p, it is easy to check that it encompasses all the particles generated by the source, $\int {\rm d}z{\rm d}p f(t, z, p) = E/p_*$, as it should, and that is contains a fraction T/p_* of the total energy:

$$\Delta E_{\rm ther} = \int {\rm d}z{\rm d}p \, |p| \, f(t, z, p) \Big|_{\rm large\ time} \simeq \frac{T}{p_*} E \quad \text{when} \quad t \gg t_{\rm br}(E) \,. \tag{4.34}$$

We thus conclude that by choosing $p_* = T$ one can ensure that the whole initial energy of the source is eventually recovered in the thermalized gluon distribution: the energy loss via viscous drag is negligible since the gluons are directly injected at the thermal scale.

5 Numerical studies of the kinetic equation

The general discussion and the parametric estimates for the energy loss presented in section 2, as well as the explicit calculations using the Green's function method in section 4.2.2, were based on an important physical assumption: the fact that the gluon cascade generated via multiple branchings is not modified by the elastic collisions responsible for thermalization and hence it can be modeled as an ideal branching process, along the lines of refs. [28, 30] — that is, a turbulent cascade, for which the medium acts as a perfect sink at the lower end ($p \sim T$) of the cascade. The validity of this assumption is far from being obvious, as shown by the following argument: via elastic collisions, the soft gluons are redistributed in phase space, in such way to match a thermal distribution, and for $p \sim T$ the latter is quite different from the scaling spectrum produced by the turbulent cascade.

In this section, we shall give up the 'perfect sink' assumption and present a detailed numerical study based on the kinetic equation (3.10). This equation too is a rather simplified version of the actual dynamics, as explained in section 3, but as compared to the source approximation in section 4 it has the merit to include an explicit infrared cutoff $p_* \sim T$ in the branching process and also the interplay between branching and thermalization at $p > p_*$.

5.1 Setting-up the problem

As in the previous section, it is convenient in practice to measure all the momenta in units of T and all the space-time scales in units of $t_{\rm rel}$, that is, to use the reduced variables

introduced in eq. (4.3). In terms of these variables, the kinetic equation (3.10) reads (with $v \equiv p/|p|$)

$$\left(\partial_t + v\partial_z\right) f(t, z, p) = \partial_p(\partial_p + v)f(t, z, p)$$

$$+ \frac{t_{\rm rel}}{t_{\rm br}(T)p^{\frac{1}{2}}} \int_r \mathrm{d}x \, \mathcal{K}(x) \left[\frac{1}{\sqrt{x}} f\left(t, z, \frac{p}{x}\right) - \frac{1}{2}f(t, z, p)\right], \qquad (5.1)$$

where we recall that the subscript r on the integral over x indicates the condition that both daughter gluons in a splitting process be harder than the 'infrared' scale $p_* \sim T$ (the lower end of the cascade). The precise kinematical conditions are as follows: for the gain term, $p > p_*$ and $p(1 - x)/x > p_*$, whereas for the loss term, $xp > p_*$ and $(1 - x)p > p_*$. For definiteness, we chose this scale p_* to be exactly equal to T (i.e. $p_* = 1$ in eq. (5.1)).

The ratio $t_{\rm rel}/t_{\rm br}(T)$ which appears in front of the branching term in eq. (5.1) is parametrically of order one for the weakly-coupled quark-gluon plasma. For what follows, it is convenient to choose this ratio to be *exactly* equal to one. This choice is also reasonable from a physics standpoint: it corresponds to the condition $\hat{q} = 16\bar{\alpha}^2 T^3$ (or, equivalently, $4\bar{\alpha}^2 T t_{\rm rel} = 1$), which is satisfied by the following values for the physical parameters:

$$\bar{\alpha} = 0.3, \quad T = 0.5 \text{ GeV}, \quad \hat{q} = 1 \text{ GeV}^2/\text{fm} \simeq 0.2 \text{ GeV}^3, \quad t_{\rm rel} = 1 \text{ fm}, \qquad (5.2)$$

which are indeed consistent with the current phenomenology.

The equation thus obtained will be solved numerically, with the initial condition

$$f(t = 0, z, p) = \delta(p - E)\delta(z) \rightarrow \frac{10}{\pi} e^{-10(p-E)^2 - 10z^2}, \qquad (5.3)$$

where the product of δ-functions is regulated as shown in the r.h.s. The picture that we expect in the light of the general discussion in section 2 is as follows:

(i) For sufficiently small times $t \ll t_{\rm br}(E)$, the leading particle should survive and carry most of the total energy. The energy lost towards the medium should be comparatively small and follow the law shown in eq. (2.6); that is, it should be of order $\omega_{\rm br}(t)$ and thus grow with t as t^2.

(ii) For larger times $t \gtrsim t_{\rm br}(E)$, the LP should disappear via democratic branching and the energy loss should be of the order of the total energy E.

For what follows, one should keep in mind that some of the assumptions underlying this picture might not be well satisfied when solving eq. (5.1) in practice. For instance, in section 2 we have assumed the medium to act as a perfect sink for the energy carried away by the branching process, which in turn allowed for a well-developed phenomenon of turbulence. This is an important hypothesis, implicitly assumed in the previous literature, for which our subsequent study will provide an explicit test.

5.2 The gluon spectrum

Before we describe the full picture of the gluon cascade in the longitudinal phase-space (z, p), let us present the results for the distribution integrated over z, that is, the gluon spectrum

$$f(t, p) \equiv \frac{\mathrm{d}N_g}{\mathrm{d}p} = \int \mathrm{d}z \, f(t, z, p) \,. \tag{5.4}$$

Clearly, this function can be obtained by solving directly the homogeneous (in the sense of independent of z) version of eq. (5.1), with initial condition $f(0, p) = \delta(p - E)$. This is a relatively simple numerical problem, which in particular allows for an extensive study of the role of the lower cutoff at $p = p_*$ on the branching process. To that aim, we shall consider three cases: (a) an 'ideal' branching process, which involves no infrared cutoff and develops a clear phenomenon of turbulence (the corresponding equation is obtained by keeping only the branching term in the r.h.s. of eq. (5.1) and letting $p_* = 0$); (b) a branching process with a sharp infrared cutoff at $p_* \ll E$, as described by eq. (5.1) without the Fokker-Planck terms, and (c) the complete dynamics (branchings with infrared cutoff p_* and elastic collisions), as described by the homogeneous version of eq. (5.1).

As already mentioned, the ideal branching process has been extensively studied in the literature and, in particular, exact analytic solutions have been obtained [28] for the case of a simplified kernel $\mathcal{K}(x) \to \mathcal{K}_0(x) \equiv 1/[x(1-x)]^{\frac{3}{2}}$. In our numerical study, we use the full kernel in eq. (3.7), but the solution is qualitatively similar to that presented in ref. [28]. Namely, for sufficiently small momenta $p \ll E$, the spectrum exhibits the scaling law $f(t, p) \propto 1/p^{3/2}$, which is a fixed point of the branching kernel and the signature of wave turbulence. For not too large times $t \ll t_{\mathrm{br}}(E)$, the leading particle is visible in the spectrum, as a pronounced peak just below $p = E$. The width of this peak increases with time (due to radiation) and eventual becomes of order one — meaning that the LP undergoes its first democratic branching — when $t \sim t_{\mathrm{br}}(E)$. For even larger times, the scaling law $\sim 1/p^{3/2}$ is still visible at small p, but the spectrum is suppressed as a whole, since the energy flows via multiple branching and accumulates at $p = 0$. When $t \gg t_{\mathrm{br}}(E)$, the whole energy E ends up in this 'condensate'. This behavior is clearly visible in the numerical results displayed in figure 7.

After introducing the infrared cutoff p_*, the gluons with $p \leq 2p_*$ cannot split anymore, as there is no phase-space available to the daughter gluons. Hence, instead of falling at $p = 0$, gluons start accumulating in the bins at $p \gtrsim p_*$. As a result, the spectrum above p_* deviates from the scaling spectrum: it shows an excess ('pile-up'), which is particularly marked at $p_* < p < 2p_*$, where it looks like a bump. Both the size of this excess and its extent in p above p_* are increasing with time, as clearly visible in figure 7. This can be understood as follows: a gluon with, say, $p = 3p_*$ has more chances to be created via the decay of parent gluons with $p \gg p_*$ (for which the kinematical constraint is relatively unimportant) than to disappear via a decay (since a significant fraction of the phase-space for its decay, that at $p \leq p_*$, is not accessible anymore).

On physical grounds, it is quite clear that this pile-up cannot be entirely physical: gluons with $p \sim T$ can efficiently lose energy towards the medium via elastic collisions and
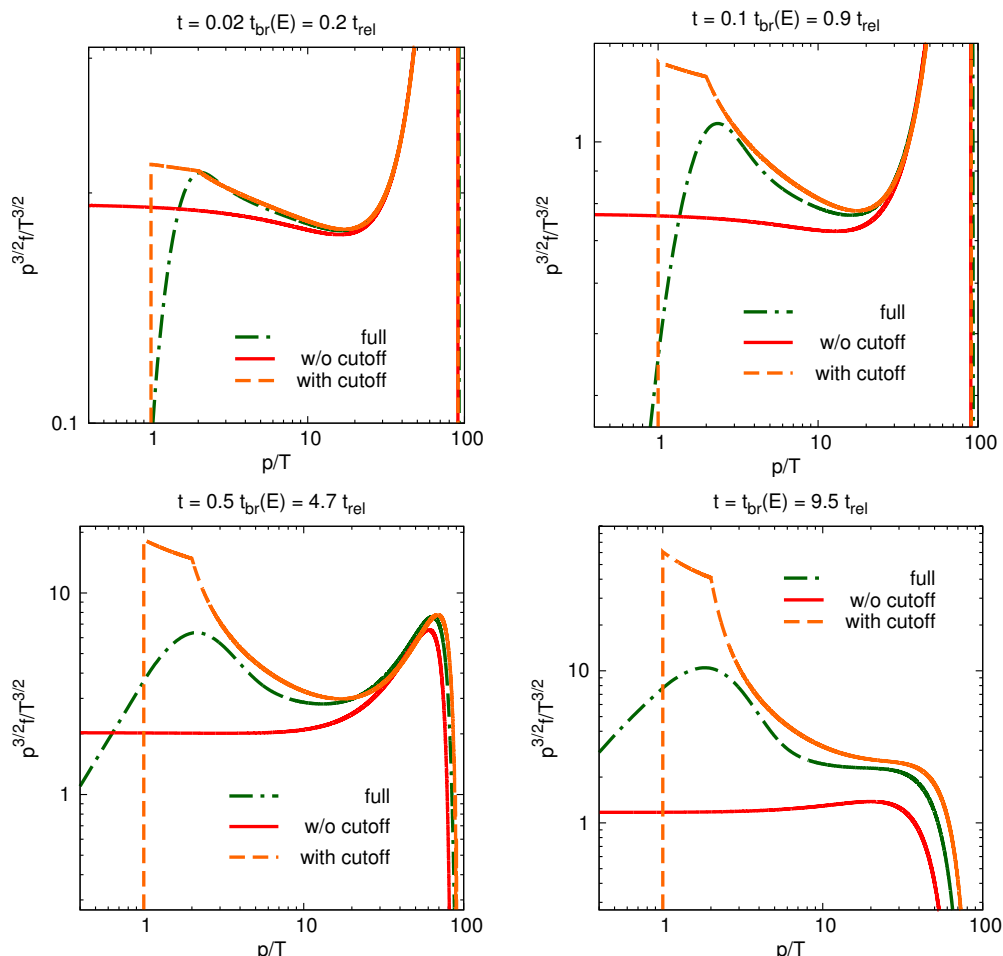
Figure 7. The gluon spectrum $f(t, p)$ for a spatially homogeneous distribution, for an initial energy $E = 90T$ and 4 values of time. The three curves correspond to (a) an ideal branching process (the red, continuous, line), (b) a branching process with infrared cutoff $p_* = T$ (orange, dotted line), and (c) the full process with branchings and elastic collisions (green, dashed-dotted line). On the vertical axis, the spectrum is multiplied by $(p/T)^{3/2}$ to render manifest the scaling behavior for the ideal branching process.

hence they should fall into the bins at lower energies $|p| < T$. We thus expect the pile-up to be considerably reduced and possibly washed out after also including the elastic collisions, as represented by the Fokker-Planck terms in the r.h.s. of eq. (5.1). This expectation is confirmed by the numerical solution to the homogeneous version of eq. (5.1) (whose results are shown too in figure 7), but only partially: the pile-up in the spectrum is indeed reduced by the elastic collisions, but the deviation with respect to the scaling spectrum remains quite large — so large, that there seems to be no scaling window in practice. If true, the last conclusion would also imply that the physical results are very sensitive to the details of the mechanism which stops the branching process and which in our analysis has been only crudely mimicked by the infrared cutoff p_*. Fortunately though, these last conclusions are not fully right and the numerical results exhibited in figure 7 are in this respect quite

misleading. The gluons which appear to accumulate on top of the scaling spectrum in this figure are actually located at *different* values of z. These are relatively soft gluons, which undergo strong diffusion as a consequence of collisions and thus separate from each other and also from the more energetic constituents of the jet (which keep propagating along the light-cone at $z = t$). Hence the 'pile-up' visible in the curves denoted as 'full' in figure 7 is merely an artifact of integrating the gluon distribution over the longitudinal coordinate z: it comes from the superposition of a nearly ideal branching spectrum in the front of the jet at $z \simeq t$ and of nearly thermal spectra in the tail of the jet at $z \ll t$. This will be demonstrated by the subsequent analysis, where the z-distribution is kept explicit.

5.3 Jet evolution in longitudinal phase-space

In this subsection we present numerical solutions to the complete equation (5.1) with initial conditions of the type shown in eq. (5.3). We consider two values for the initial energy, $E = 25\,T$ and $E = 90\,T$, which correspond to rather distinct physical situations. The first value $E = 25\,T$ ($= 12.5\,\text{GeV}$ according to eq. (5.2)) is quite low and is representative for a *mini-jet* radiated by a leading particle with a much higher energy $E_0 \geq 100\,\text{GeV}$. This is one of the typical mini-jets which control the energy loss in the case where the LP crosses the medium along a distance $L \simeq t_{\text{br}}(E) = 5\,t_{\text{rel}} = 5\,\text{fm}$. The second value $E = 90\,T = 45\,\text{GeV}$ is closer to the energy of an actual jet at the LHC and in particular is large enough to ensure that the respective leading particle does not disappear into the medium: indeed, the respective branching time $t_{\text{br}}(E) \simeq 9.5\,\text{fm}$ is larger than the typical distance $L \lesssim 8\,\text{fm}$ that the LP might travel across the medium in the experimental situation at the LHC.
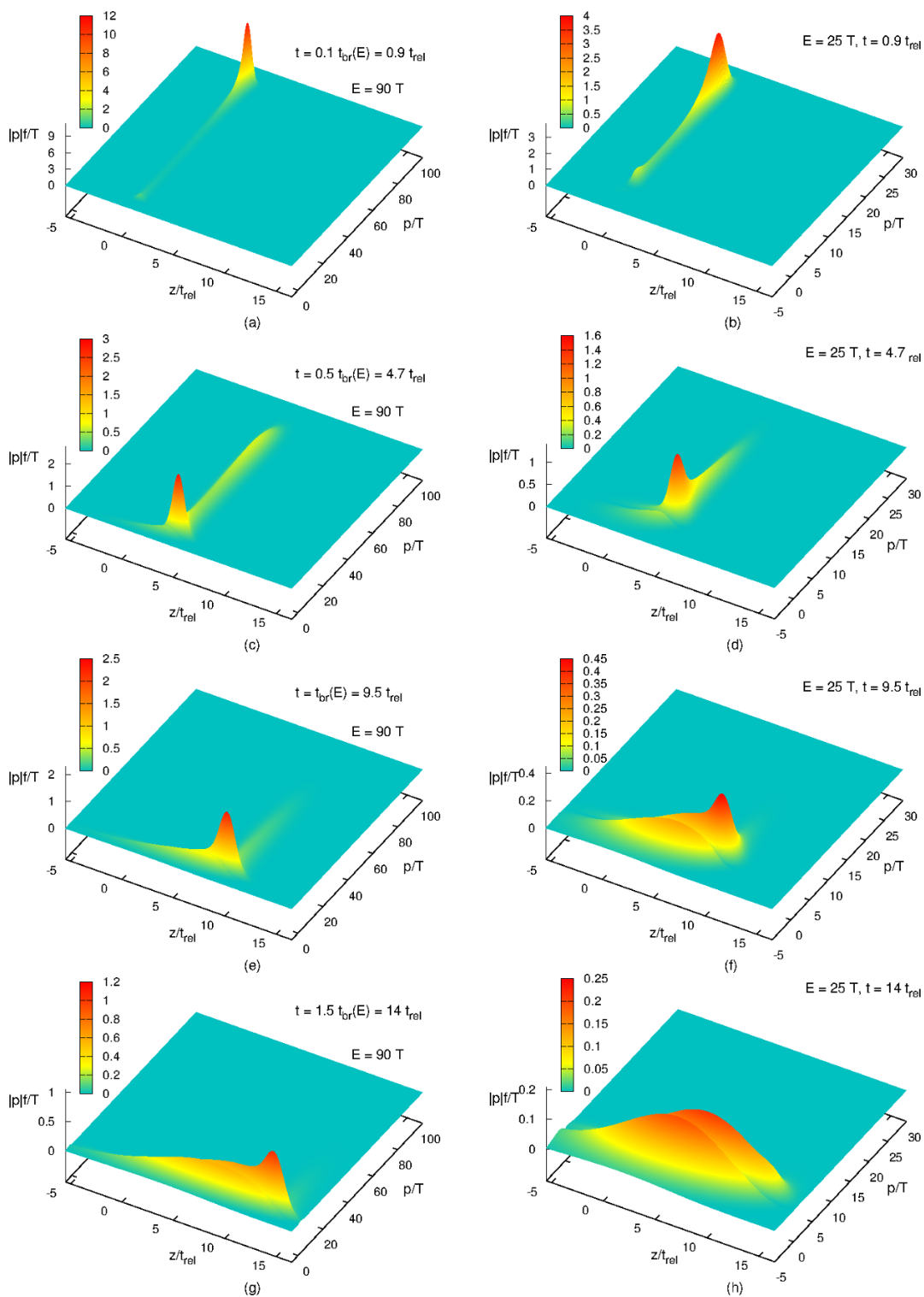
5.3.1 The gluon distribution and the energy density

The general features of the evolution of the gluon cascade produced by a high-energy jet can be appreciated by inspection of figures 8 and 9, which show the phase-space distribution of the gluon number $f(t, z, p)$ and, respectively, the gluon energy $|p| f(t, z, p)$, for the two energies of the LP, $E = 90\,T$ and $25\,T$, and four values of time: $t/t_{\text{rel}} = 0.95, 4.7, 9.5$, and 14. These particular values for t have been chosen since, with our present conventions (i.e. $t_{\text{br}}(E)/t_{\text{rel}} = \sqrt{E/T}$), they correspond to rather special values for the case of a jet with $E = 90\,T$; namely, they amount to $t/t_{\text{br}}(90) \simeq 0.1, 0.5, 1$, and 1.5, respectively. Since the natural time scale for the jet evolution is $t_{\text{br}}(E)$, let us also list the corresponding values for the softer jet with $E = 25\,T$: one roughly has $t/t_{\text{br}}(25) \simeq 0.2, 1, 2$, and 3, respectively. To gain more intuition about these time scales in physical units, it is useful to recall that $t_{\text{rel}} = 1\,\text{fm}$ for the medium parameters in eq. (5.2).

When discussing figures 8 and 9, it is natural to group together those plots which correspond to different values of the energy E, but similar values of $t/t_{\text{br}}(E)$, because they refer to similar stages in the evolution of the jet via branching. But even for identical values of $t/t_{\text{br}}(E)$, one should still expect some differences between the two cases, $E = 90\,T$ and $E = 25\,T$, because the physics of thermalization introduces an additional energy scale in the problem — the infrared cutoff p_*.
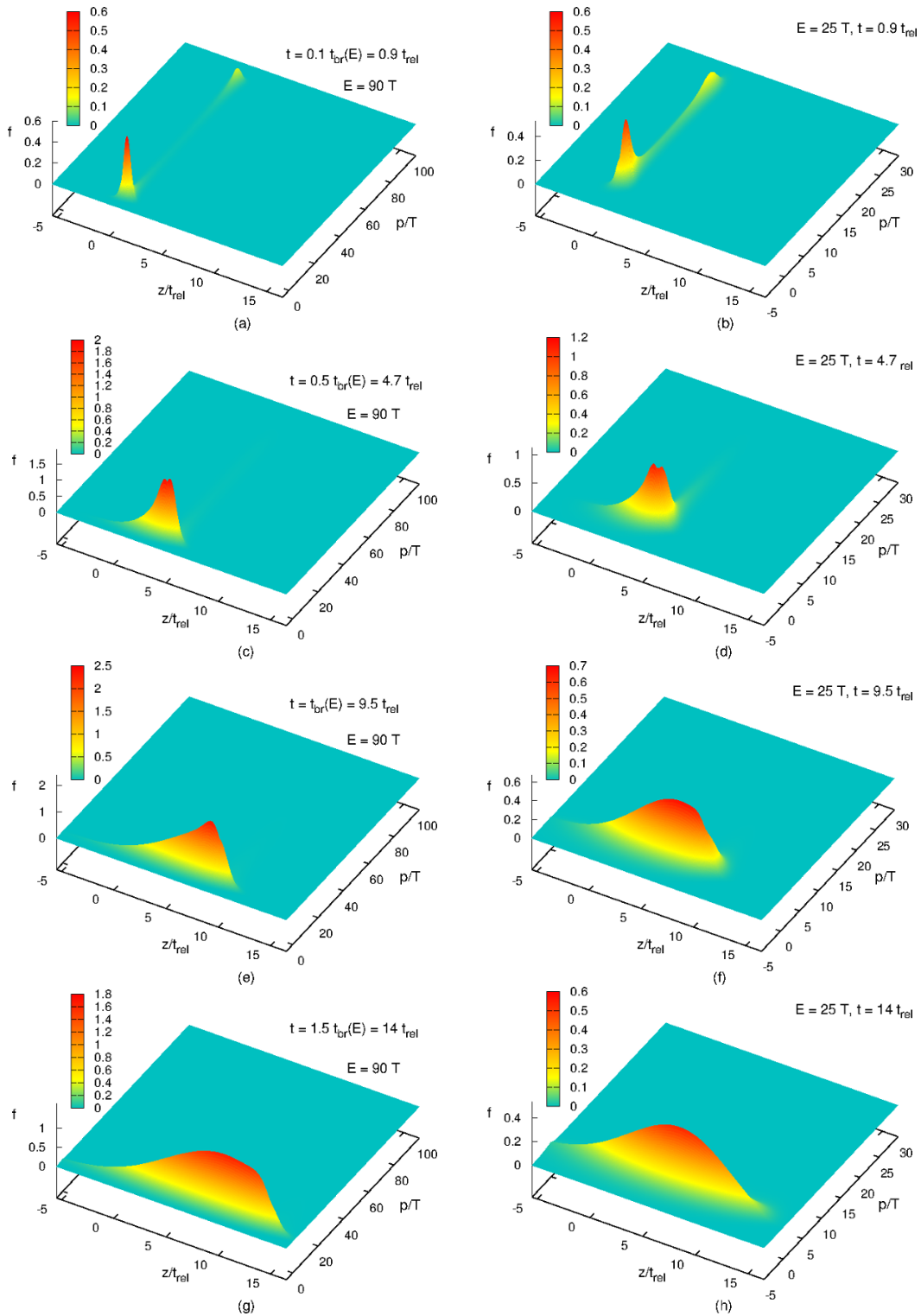
Figure 8. The time evolution of the phase-space distribution $f(t, z, p)$ produced by a jet with initial energy $E = 90\,T$ (left) and respectively $E = 25\,T$ (right), plotted for exactly the same values of time.

**Figure 9**. The time evolution of the phase-space energy density $|p|f/T$, for the same conditions as in figure 8.
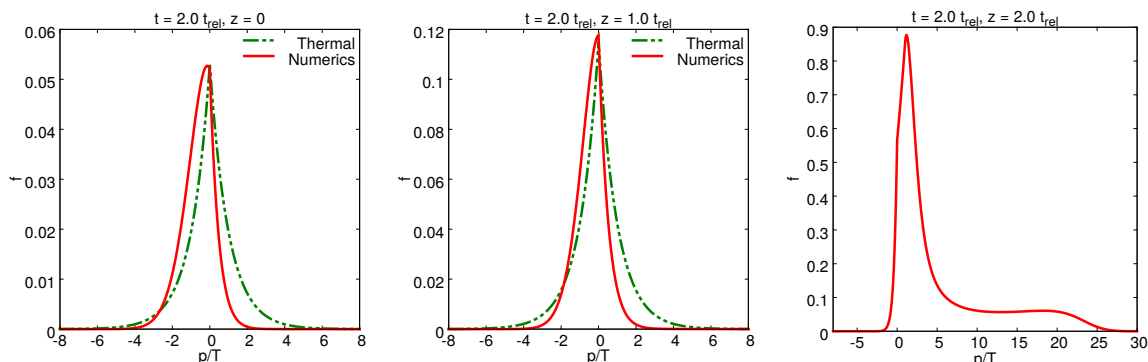
Figure 10. The gluon distribution $f(t, z, p)$ for $E = 25\,T$ is represented as a function of p at time $t = 2t_{\mathrm{rel}}$ and for 3 different values of z: $z = 0$, $z = t_{\mathrm{rel}}$, and $z = 2t_{\mathrm{rel}}$. For $z < t - t_{\mathrm{rel}}$, the momentum distribution is nearly thermal, but with an overall strength which depends upon z: $f(z, p) \simeq f_0(z)\mathrm{e}^{-|p|/T}$. For $z = t$ on the other hand, the distribution is far from thermal equilibrium, albeit it is still strongly peaked near $p = T$. Similar conclusions hold for the distribution at later times and for a jet with $E = 90\,T$.

Consider first figures 8 (a)-(c) and figures 9 (a)-(c), which illustrate the evolution at early stages, $t < t_{\mathrm{br}}(E)$. Figures 8 (a)-(c) show that, already for such early times, most of the particles are relatively soft ($p \sim p_* = T$), meaning that they are products of radiation. In particular, those particles which at a given time t have an energy $|p|$ smaller than $\omega_{\mathrm{br}}(t) = \bar{\alpha}^2 \hat{q} t^2$, are generally produced via *multiple branchings*, that is, they belong to gluon cascades generated via democratic branchings by primary gluons with $p \sim \omega_{\mathrm{br}}(t)$. But so long as $t \ll t_{\mathrm{br}}(E)$, most of the energy is still carried by the LP, as manifest in figures 9 (a)-(b): the energy distribution is peaked at a value which is smaller than, but comparable to, the original energy E. When $t_{\mathrm{rel}} \lesssim t \ll t_{\mathrm{br}}(E)$, the energy loss by the LP and its longitudinal broadening are both controlled by soft branchings and hence they grow with time like t^2.

Figure 9 (c) shows another interesting feature: for $t \simeq 0.5\,t_{\mathrm{br}}(E)$, one sees a second peak emerging in the energy distribution at $p \sim T$. This demonstrates the strong accumulation of gluons towards the lower end of the spectrum which in turn reflects a limitation of the medium capacity to act as a 'perfect sink'. We shall later return to a more detailed study of this phenomenon (see notably figures 11 and 13 and the associated discussions).

As also visible in figures 8 (a)-(c), the approach to thermalization in the tail of the distribution at $z < t$ is noticeable already at such early times $t < t_{\mathrm{br}}(E)$. There is indeed a substantial number of gluons which remain behind the LP (i.e., which do not travel at the speed of light) and whose momentum distribution is nearly thermal. This is more clearly illustrated by the plots in figure 10, corresponding to $E = 25\,T$, which show the momentum distribution at $t = 2\,t_{\mathrm{rel}} = 0.4\,t_{\mathrm{br}}(25)$ and for different values of z: the shape of this distribution is close to the exponential $\mathrm{e}^{-|p|/T}$ at any $z \lesssim t - t_{\mathrm{rel}}$.

Consider now later times $t \gtrsim t_{\mathrm{br}}(E)$, where one expects the LP to disappear via democratic branching. Figures 9 (d) and (e) confirm that, when $t \sim t_{\mathrm{br}}(E)$, there is no visible trace of the LP, albeit a few semi-hard particles, with $T \ll p \ll E$, still exist.
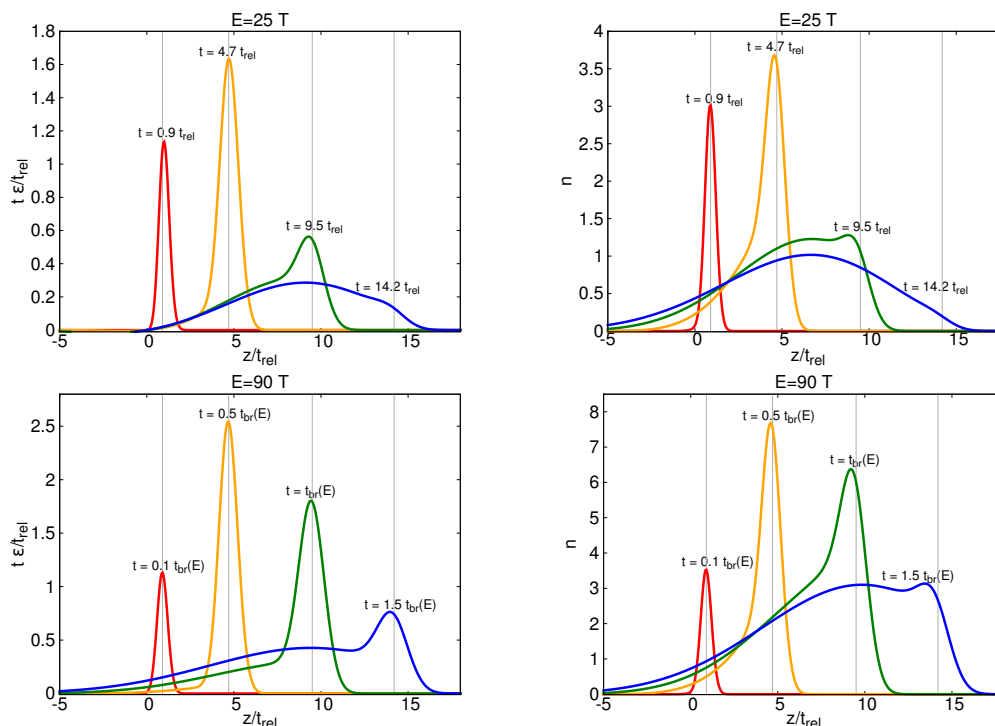
Figure 11. The energy density and the gluon number density are shown as functions of z at different times. The grey vertical lines indicate the location of the light-cone, that is, $z = t$, for each value of t.

For even larger times, these semi-hard particles will themselves disappear via democratic branchings, so there will be an increasing fraction of the total energy which is carried by the soft gluons with $p \lesssim T$. This trend is indeed visible in figures 9 (f)-(h). However, one should not conclude that all this energy has already thermalized: the soft gluons which propagate together with their (semi-)hard sources along the light-cone $z = t$ cannot be thermal. This is already illustrated by the last plot in figure 10: the momentum distribution corresponding to $z = t = 2\,t_{\mathrm{rel}}$ is peaked at small $p \sim T$, yet it strongly deviates from a thermal distribution.

To better distinguish between thermal and non-thermal (soft) gluons at late times, we have exhibited in figure 11 the z-distribution of the energy and number densities, defined as

$$\varepsilon(t,z) = \int \mathrm{d}p\,|p|\,f(t,z,p)\,, \qquad n(t,z) = \int \mathrm{d}p\,f(t,z,p)\,. \tag{5.5}$$

As visible in these plots, even for times as large as $t = 1.5\,t_{\mathrm{br}}(E)$, where we know (say, from figures 9 (f) and (g)) that the energy is preponderantly carried by soft quanta with $p \sim T$, the energy distribution is still strongly peaked at $z = t$, meaning that most of these soft gluons are *not* thermal: they have been emitted at late stages and did not have the time to thermalize. This finding is in agreement with the discussion following eq. (4.29), where we noticed that the flux of soft gluons is largest towards the late stages of the cascade. The situation changes at the larger time $t = 3\,t_{\mathrm{br}}(E)$, that we can here access only for
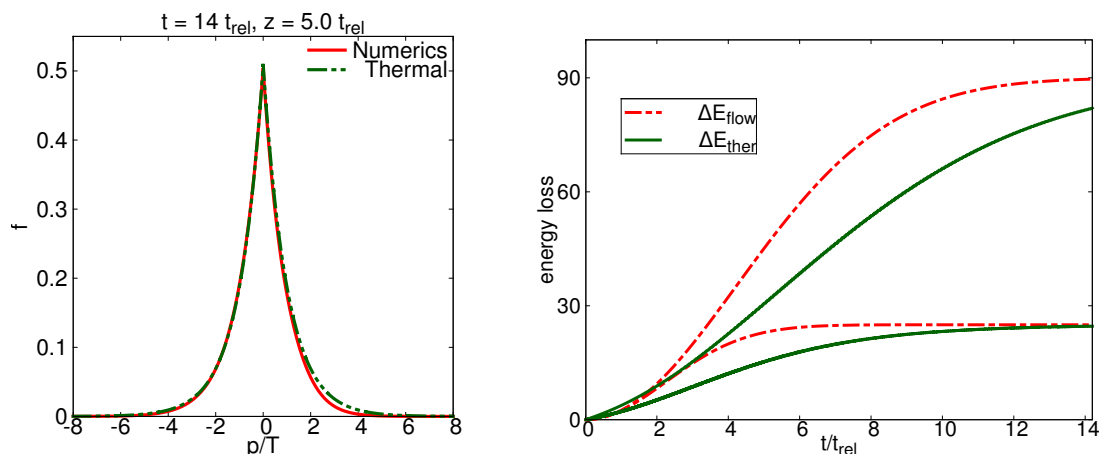
Figure 12. Left: the gluon distribution $f(t, z, p)$ for $E = 25\,T$ is plotted as a function of p for $t = 14.2\,t_{\mathrm{rel}} \simeq 3t_{\mathrm{br}}(E)$ and $z = t_{\mathrm{br}}(E) = 5\,t_{\mathrm{rel}}$ and compared to a thermal distribution with the same normalization at $p = 0$. Right: the energy loss towards the medium $\Delta E_{\mathrm{ther}}(t)$ (in units of T), eq. (5.6), plotted as a function t for $E = 25\,T$ and $E = 90\,T$. The result is compared to the flow energy (4.29) which applies to an ideal cascade.

the jet with $E = 25\,T$ (by looking at $t = 14.2\,t_{\mathrm{rel}} \simeq 3\,t_{\mathrm{br}}(25)$). In that case, we see that both densities, $\varepsilon(t, z)$ and $n(t, z)$, peak well behind the light-cone — in particular, the number distribution peaks around $z \simeq t_{\mathrm{br}}(E) = 5\,t_{\mathrm{rel}}$, in agreement with eq. (4.33). This strongly indicates that the entire gluon distribution produced by the jet has thermalized by $t = 3\,t_{\mathrm{br}}(E)$: the jet is *fully quenched*. This conclusion can be also checked by plotting the distribution $f(t, z, p)$ as a function of p for $t = 3\,t_{\mathrm{br}}(E)$ and, say, $z = t_{\mathrm{br}}(E)$: this is shown in figure 12 (left) which indeed features an almost perfect thermal distribution. The distribution of such a fully quenched jet in longitudinal phase-space is illustrated by figures 8 (h) and 9 (h). Clearly, this is very similar to the late-time distributions found in section 4, cf. figures 5 and 3: a distribution symmetric in z which extends via diffusion.

5.3.2 Energy loss towards the medium

Given our previous numerical results, it is furthermore interesting to use them to extract the energy lost by the jet towards the medium. A priori, this involves two components: the energy dissipated into the medium via the drag force (physically, this is the energy transferred to the plasma constituents through elastic collisions) and the energy taken away by the gluons from the jet which have reached a thermal distribution in momentum (since such gluons cannot be distinguished from the medium constituents anymore). As noticed at the end of section 4.2.2, the drag component can be minimized by choosing $p_* = T$, so it should be enough to compute the energy carried by the thermalized part of the gluon distribution. Still, to avoid any uncertainty concerning the contribution of the drag, it is preferable to compute the energy loss as the *difference* between the original energy E of the LP and the energy carried by the jet constituents which have *not* thermalized. This definition too is a bit ambiguous though, because the distinction between thermal and non-thermal gluons is not really sharp, as already noticed. Yet, we have seen that the

gluons in the tail of the distribution at $z \lesssim t - t_{\rm rel}$ are approximately thermal, whereas those which belong to the front ($z > t - t_{\rm rel}$) are still far away from thermal equilibrium — at least for not too late time, $t \lesssim t_{\rm br}(E)$, when the front still exist (see e.g. figure 10). This observation motivates the following definition for the energy loss via thermalization:

$$\Delta E_{\rm ther}(t) = E - \int_{t-t_{\rm rel}}^{\infty} {\rm d}z \int_{p_*}^{\infty} {\rm d}p \, p \, f(t, z, p) \,. \tag{5.6}$$

For sufficiently large times $t \gg t_{\rm br}(E)$, all the gluons lie $z < t - t_{\rm rel}$ (the front disappears) and $\Delta E_{\rm ther} \simeq E$. But the most interesting situation for the LHC, is when the medium size L is small relative to the branching time $t_{\rm br}(E)$ for the LP, hence $\Delta E_{\rm ther}$ is small compared to E.

In the right hand side of figure 12 we present our numerical results for $\Delta E_{\rm ther}(t)$ as a function of t (or, equivalently, the medium size) for the two energies of interest, $E = 25\,T$ and $E = 90\,T$. For comparison, we also show the corresponding prediction $\Delta E_{\rm flow}(t)$ of eq. (4.29); this would be the energy transferred to the medium in the ideal case where the plasma acts as a perfect absorber for the gluons with $p \lesssim T$ (without affecting the branching dynamics at $p > T$). Not surprisingly, the energy loss $\Delta E_{\rm ther}(t)$ for the 'physical' cascade remains significantly lower than the 'ideal' expectation $\Delta E_{\rm flow}(t)$ for all times $t \lesssim t_{\rm br}(E)$, that is, so long as the gluon cascade has not fully thermalized. (For large times $t \gg t_{\rm br}(E)$, these two quantities approach to each other, as they both converge towards the total energy E, as they should.) The main reason for this discrepancy is the fact that the medium is *not* a perfect sink: there is a delay in the thermalization of the soft gluons produced via branchings and, as a result, gluons with $p \sim T$ can still propagate at the speed of light over a time interval $\Delta t \gtrsim t_{\rm rel}$ after their production. Since the production rate increases with time, cf. eq. (4.29), it is natural that the difference between $\Delta E_{\rm flow}(t)$ and $\Delta E_{\rm ther}(t)$ increases as well so long as the LP still exists, i.e. for $t \lesssim t_{\rm br}(E)$. This trend is indeed visible in figure 12 (right).

This being said, the energy loss $\Delta E_{\rm ther}$ that we have numerically found is significantly large. By inspection of figure 12, we see that $\Delta E_{\rm ther}(L) \simeq 30\,T \, (= 15\,{\rm GeV})$ for a jet with $E = 90\,T \, (= 45\,{\rm GeV})$ and for a medium size $L = 5\,t_{\rm rel} \, (= 5\,{\rm fm})$. Furthermore, as also visible in figure 12, the energy loss rises quite fast with time and hence with the medium size L: at small times $t \ll t_{\rm br}(E)$, one roughly has $\Delta E_{\rm ther}(t) \propto t^2$, in agreement with eq. (2.6), whereas for larger times $t \gtrsim t_{\rm br}(E)$, $\Delta E_{\rm ther}(t)$ approaches the total energy E of the LP: the jet is 'fully quenched'.

Whereas the results in figure 12 (right) point out towards a failure of the hypothesis of a 'perfect sink', this failure remains quite mild, especially at early times $t \ll t_{\rm br}(E)$. This is already suggested by the qualitative similarity between the gluon distribution produced by a 'real' jet, as shown in figure 8, and that generated by an ideal gluon cascade, cf. figure 3 and figure 6. To have a more quantitative test in that sense, we have studied the gluon spectrum near the front of the jet, that is, the distribution $f(t, z, p)$ produced by the kinetic equation at $z = t$. At small times $t \lesssim 0.5t_{\rm br}(E)$, the numerical results in figure 13 exhibit a relatively wide window at $T < p \ll E$ where the front distribution function shows the same scaling behavior, $f(z = t, p) \propto 1/p^{3/2}$, as the ideal branching process (compare to
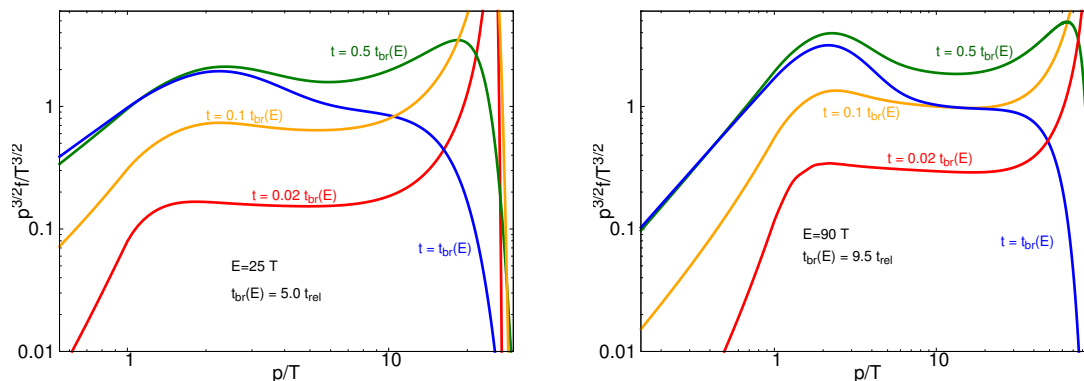
Figure 13. The gluon distribution in momentum at $t = z$ for two energies, $E = 25\,T$ and $E = 90\,T$, and for 4 values of time, which are now chosen to be the same in units of $t_{\rm br}(E)$ for both energies. The figures show a rather broad window of approximate scaling behavior, $f \propto 1/p^{3/2}$, at not too large times $t \lesssim t_{\rm br}(E)$.

the curved 'w/o cutoff' in figure 7). As repeatedly stressed, this scaling law is a hallmark of wave turbulence. Figure 13 should be contrasted to the corresponding results for the spectrum $f(t, p) = \int \mathrm{d}z f(t, z, p)$ (the curves denoted as 'full' in figure 7), which show no scaling window at all. So, in this respect at least, the gluon spectrum is potentially misleading, as anticipated in section 5.2.

More generally, the ensemble of studies that we have performed in this paper demonstrate that the detailed phase-space distribution is better suited than the gluon spectrum for understanding the in-medium evolution of the jets.

6 Conclusions and perspectives

In this paper, we have presented a first study of the thermalization of the soft components of the gluon cascades generated via multiple branchings by an energetic parton which propagates through a weakly-coupled quark-gluon plasma. Our overall picture is rather simple and physically motivated, and in our opinion it is also quite robust: indeed, this picture is almost an immediate consequence of the strong separation of scales between the characteristic time for the medium-induced branchings of hard gluons and, respectively, the relaxation time for the thermalization of soft gluons. In trying to establish this picture beyond parameter estimates, we met with several difficulties and subtle points, for which we proposed at least partial solutions.

A major difficulty is the overall complexity of the problem, that we have tried to circumvent via suitable approximations, notably by carefully separating the gluons from the jet from those in the medium and by projecting the dynamics onto the one-dimensional, longitudinal, phase-space. These approximations are fully justified for the sufficiently hard gluons in the cascades, with momenta $p \gg T$, which control the dynamics of multiple branchings. On the other hand, these approximations becomes less justified when moving to the softer gluons with $p \lesssim T$, where they are at most qualitatively right. (But we have tried to carefully argue that they correctly reproduce the relevant time scales to parametric accuracy.) A particularly subtle approximation refers to the branching dynamics near the

lower end of the cascades, at $p \sim T$, where we expect the cascade to terminate, on physical grounds. In our calculations, we have simply cut off the branching process at a scale $p_* \sim T$ and found that, thanks to the smearing effect of the elastic collisions, the results are not very sensitive to the precise value of this cutoff. (We have indeed checked that our numerical results remain qualitatively and even semi-quantitatively unchanged when varying this cutoff by a factor of 2 around its central value.) But it would be of course important, both conceptually and phenomenologically, to have a dynamical implementation of this cutoff, which in turn requires a consistent treatment of the full gluon distribution at soft momenta, including the inherent non-linear effects.

This discussion points towards the many 'technical' limitations in our approach, with potential physical consequences, which will be hopefully lifted by more detailed, future, analyses. In principle, the theoretical framework for such studies is well defined: this is set by the general kinetic equations alluded to in section 3, that can be found in the literature [36, 44]. A main difficulty as compared to previous numerical studies of such equations in the literature [39, 51, 52], is that fact that, for the jet problem at hand, one needs to explicitly deal with the strong spatial inhomogeneity introduced by the hard components of the jet.

Another interesting direction of research refers to a better understanding of the implications of the present picture for the phenomenology of jets in heavy ion collisions at RHIC and the LHC. Our first estimates for the energy loss via thermalization, which are of course very raw and must be taken with a grain of salt, are quite encouraging in that sense. In our opinion, it makes sense to compare, at least qualitatively, the quantity ΔE_{ther} introduced in eq. (5.6) (the energy carried away by the thermalized gluons in the tail of the jet) with the energy imbalance at large angles, as measured in the context of the di-jet asymmetry. The detailed analyses of the corresponding data, notably by the CMS collaboration [20, 26], demonstrate that the energy imbalance is carried by an excess of soft hadrons ($p_T \lesssim 2\,\text{GeV}$) propagating at large angles. It looks natural to associate these soft hadrons with the 'thermalized gluons' in our current set-up. If so, it is interesting to notice that our estimates for ΔE_{ther} in figure 12 (right) are in the ballpark of 10 to 20 GeV (for $E = 90\,T$ and physically interesting values of the medium size L), which is not unreasonable for the phenomenology alluded to above. But of course further studies, to remove some of our theoretical uncertainties and to better defines experimental observables, are still needed before aiming at a detailed comparison with the phenomenology.

Acknowledgments

References

[1] M. Gyulassy and X.-n. Wang, *Multiple collisions and induced gluon Bremsstrahlung in QCD*, *Nucl. Phys.* **B 420** (1994) 583 [nucl-th/9306003] [INSPIRE].

[2] R. Baier, Y.L. Dokshitzer, A.H. Mueller, S. Peigne and D. Schiff, *Radiative energy loss of high-energy quarks and gluons in a finite volume quark-gluon plasma*, *Nucl. Phys.* **B 483** (1997) 291 [hep-ph/9607355] [INSPIRE].

[3] R. Baier, Y.L. Dokshitzer, A.H. Mueller, S. Peigne and D. Schiff, *Radiative energy loss and p_T broadening of high-energy partons in nuclei*, *Nucl. Phys.* **B 484** (1997) 265 [hep-ph/9608322] [INSPIRE].

[4] B.G. Zakharov, *Fully quantum treatment of the Landau-Pomeranchuk-Migdal effect in QED and QCD*, *JETP Lett.* **63** (1996) 952 [hep-ph/9607440] [INSPIRE].

[5] B.G. Zakharov, *Radiative energy loss of high-energy quarks in finite size nuclear matter and quark-gluon plasma*, *JETP Lett.* **65** (1997) 615 [hep-ph/9704255] [INSPIRE].

[6] R. Baier, Y.L. Dokshitzer, A.H. Mueller and D. Schiff, *Medium induced radiative energy loss: Equivalence between the BDMPS and Zakharov formalisms*, *Nucl. Phys.* **B 531** (1998) 403 [hep-ph/9804212] [INSPIRE].

[7] U.A. Wiedemann, *Gluon radiation off hard quarks in a nuclear environment: Opacity expansion*, *Nucl. Phys.* **B 588** (2000) 303 [hep-ph/0005129] [INSPIRE].

[8] U.A. Wiedemann, *Jet quenching versus jet enhancement: A quantitative study of the BDMPS-Z gluon radiation spectrum*, *Nucl. Phys.* **A 690** (2001) 731 [hep-ph/0008241] [INSPIRE].

[9] P.B. Arnold, G.D. Moore and L.G. Yaffe, *Photon emission from ultrarelativistic plasmas*, *JHEP* **11** (2001) 057 [hep-ph/0109064] [INSPIRE].

[10] P.B. Arnold, G.D. Moore and L.G. Yaffe, *Photon emission from quark gluon plasma: Complete leading order results*, *JHEP* **12** (2001) 009 [hep-ph/0111107] [INSPIRE].

[11] P.B. Arnold, G.D. Moore and L.G. Yaffe, *Photon and gluon emission in relativistic plasmas*, *JHEP* **06** (2002) 030 [hep-ph/0204343] [INSPIRE].

[12] R. Baier, D. Schiff and B.G. Zakharov, *Energy loss in perturbative QCD*, *Ann. Rev. Nucl. Part. Sci.* **50** (2000) 37 [hep-ph/0002198] [INSPIRE].

[13] J. Casalderrey-Solana and C.A. Salgado, *Introductory lectures on jet quenching in heavy ion collisions*, *Acta Phys. Polon.* **B 38** (2007) 3731 [arXiv:0712.3443] [INSPIRE].

[14] Y. Mehtar-Tani, J.G. Milhano and K. Tywoniuk, *Jet physics in heavy-ion collisions*, *Int. J. Mod. Phys.* **A 28** (2013) 1340013 [arXiv:1302.2579] [INSPIRE].

[15] D. d'Enterria, *Jet quenching*, *Landolt-Bornstein* **23** (2010) 471 [arXiv:0902.2011] [INSPIRE].

[16] A. Majumder and M. Van Leeuwen, *The Theory and Phenomenology of Perturbative QCD Based Jet Quenching*, *Prog. Part. Nucl. Phys.* **A 66** (2011) 41 [arXiv:1002.2206] [INSPIRE].

[17] JET collaboration, K.M. Burke et al., *Extracting the jet transport coefficient from jet quenching in high-energy heavy-ion collisions*, *Phys. Rev.* **C 90** (2014) 014909 [arXiv:1312.5003] [INSPIRE].

[18] G. Roland, K. Safarik and P. Steinberg, *Heavy-ion collisions at the LHC*, *Prog. Part. Nucl. Phys.* **77** (2014) 70 [INSPIRE].

[19] ATLAS collaboration, *Observation of a Centrality-Dependent Dijet Asymmetry in Lead-Lead Collisions at $\sqrt{s_{NN}} = 2.77\,TeV$ with the ATLAS Detector at the LHC*, *Phys. Rev. Lett.* **105** (2010) 252303 [arXiv:1011.6182] [INSPIRE].

[20] CMS collaboration, *Observation and studies of jet quenching in PbPb collisions at nucleon-nucleon center-of-mass energy = 2.76 TeV*, *Phys. Rev.* **C 84** (2011) 024906 [arXiv:1102.1957] [INSPIRE].

[21] CMS collaboration, *Jet momentum dependence of jet quenching in PbPb collisions at $\sqrt{s_{NN}} = 2.76\,TeV$*, *Phys. Lett.* **B 712** (2013) 176 [arXiv:1202.5022] [INSPIRE].

[22] ATLAS collaboration, *Measurement of the jet radius and transverse momentum dependence of inclusive jet suppression in lead-lead collisions at $\sqrt{s_{NN}} = 2.76\,TeV$ with the ATLAS detector*, *Phys. Lett.* **B 719** (2013) 220 [arXiv:1208.1967] [INSPIRE].

[23] CMS collaboration, *Modification of jet shapes in PbPb collisions at $\sqrt{s_{NN}} = 2.76\,TeV$*, *Phys. Lett.* **B 730** (2014) 243 [arXiv:1310.0878] [INSPIRE].

[24] CMS collaboration, *Measurement of jet fragmentation in PbPb and pp collisions at $\sqrt{s_{NN}} = 2.76\,TeV$*, *Phys. Rev.* **C 90** (2014) 024908 [arXiv:1406.0932] [INSPIRE].

[25] ATLAS collaboration, *Measurement of inclusive jet charged-particle fragmentation functions in Pb+Pb collisions at $\sqrt{s_{NN}} = 2.76\,TeV$ with the ATLAS detector*, *Phys. Lett.* **B 739** (2014) 320 [arXiv:1406.2979] [INSPIRE].

[26] CMS collaboration, *Measurement of transverse momentum flow relative to the dijet system in PbPb and pp collisions at $\sqrt{s_{NN}} = 2.76\,TeV$*, CMS-PAS-HIN-14-010 (2014).

[27] J.-P. Blaizot, F. Dominguez, E. Iancu and Y. Mehtar-Tani, *Medium-induced gluon branching*, *JHEP* **01** (2013) 143 [arXiv:1209.4585] [INSPIRE].

[28] J.-P. Blaizot, E. Iancu and Y. Mehtar-Tani, *Medium-induced QCD cascade: democratic branching and wave turbulence*, *Phys. Rev. Lett.* **111** (2013) 052001 [arXiv:1301.6102] [INSPIRE].

[29] J.-P. Blaizot, F. Dominguez, E. Iancu and Y. Mehtar-Tani, *Probabilistic picture for medium-induced jet evolution*, *JHEP* **06** (2014) 075 [arXiv:1311.5823] [INSPIRE].

[30] L. Fister and E. Iancu, *Medium-induced jet evolution: wave turbulence and energy loss*, *JHEP* **03** (2015) 082 [arXiv:1409.2010] [INSPIRE].

[31] A. Kurkela and U.A. Wiedemann, *Picturing perturbative parton cascades in QCD matter*, *Phys. Lett.* **B 740** (2015) 172 [arXiv:1407.0293] [INSPIRE].

[32] J.-P. Blaizot, Y. Mehtar-Tani and M.A.C. Torres, *Angular structure of the in-medium QCD cascade*, *Phys. Rev. Lett.* **114** (2015) 222002 [arXiv:1407.0326] [INSPIRE].

[33] L. Apolinário, N. Armesto, J.G. Milhano and C.A. Salgado, *Medium-induced gluon radiation and colour decoherence beyond the soft approximation*, *JHEP* **02** (2015) 119 [arXiv:1407.0599] [INSPIRE].

[34] J.-P. Blaizot, L. Fister and Y. Mehtar-Tani, *Angular distribution of medium-induced QCD cascades*, *Nucl. Phys.* **A 940** (2015) 67 [arXiv:1409.6202] [INSPIRE].

[35] J.-P. Blaizot and Y. Mehtar-Tani, *Energy flow along the medium-induced parton cascade*, arXiv:1501.03443 [INSPIRE].

[36] R. Baier, A.H. Mueller, D. Schiff and D.T. Son, *'Bottom up' thermalization in heavy ion collisions*, *Phys. Lett.* **B 502** (2001) 51 [hep-ph/0009237] [INSPIRE].

[37] R. Baier, Y.L. Dokshitzer, A.H. Mueller and D. Schiff, *Quenching of hadron spectra in media*, *JHEP* **09** (2001) 033 [hep-ph/0106347] [INSPIRE].

[38] S. Jeon and G.D. Moore, *Energy loss of leading partons in a thermal QCD medium*, *Phys. Rev.* **C 71** (2005) 034901 [hep-ph/0309332] [INSPIRE].

[39] B. Schenke, C. Gale and S. Jeon, *MARTINI: An event generator for relativistic heavy-ion collisions*, *Phys. Rev.* **C 80** (2009) 054913 [arXiv:0909.2037] [INSPIRE].

[40] J.-P. Blaizot and Y. Mehtar-Tani, *Jet Structure in Heavy Ion Collisions*, arXiv:1503.05958 [INSPIRE].

[41] A. Kurkela and G.D. Moore, *Thermalization in Weakly Coupled Nonabelian Plasmas*, *JHEP* **12** (2011) 044 [arXiv:1107.5050] [INSPIRE].

[42] V. Zakharov, V. Lvov and G. Falkovich, *Kolmogorov spectra of turbulence I*, Springer-Verlag, (1992), pg. 264.

[43] S. Nazarenko, *Wave Turbulence*, Springer-Verlag, (2011), pg. 279.

[44] P.B. Arnold, G.D. Moore and L.G. Yaffe, *Effective kinetic theory for high temperature gauge theories*, *JHEP* **01** (2003) 030 [hep-ph/0209353] [INSPIRE].

[45] E. Lifshitz and L. Pitaevskii, *Physical Kinetics*, Pergamon Press, New York, (1981).

[46] G.D. Moore and D. Teaney, *How much do heavy quarks thermalize in a heavy ion collision?*, *Phys. Rev.* **C 71** (2005) 064904 [hep-ph/0412346] [INSPIRE].

[47] R. Rapp and H. van Hees, *Heavy Quarks in the quark-gluon Plasma*, arXiv:0903.1096 [INSPIRE].

[48] J. Ghiglieri and D. Teaney, *Parton energy loss and momentum broadening at NLO in high temperature QCD plasmas*, arXiv:1502.03730 [INSPIRE].

[49] J.-P. Blaizot, B. Wu and L. Yan, *Quark production, Bose-Einstein condensates and thermalization of the quark-gluon plasma*, *Nucl. Phys.* **A 930** (2014) 139 [arXiv:1402.5049] [INSPIRE].

[50] P.B. Arnold, G.D. Moore and L.G. Yaffe, *Transport coefficients in high temperature gauge theories. 2. Beyond leading log*, *JHEP* **05** (2003) 051 [hep-ph/0302165] [INSPIRE].

[51] A. Kurkela and E. Lu, *Approach to Equilibrium in Weakly Coupled Non-Abelian Plasmas*, *Phys. Rev. Lett.* **113** (2014) 182301 [arXiv:1405.6318] [INSPIRE].

[52] A. Kurkela and Y. Zhu, *Isotropization and hydrodynamization in weakly coupled heavy-ion collisions*, arXiv:1506.06647 [INSPIRE].

[53] X.-G. Huang and J. Liao, *Kinetic evolution of the glasma and thermalization in heavy ion collisions*, *Int. J. Mod. Phys.* **E 23** (2014) 1430003 [arXiv:1402.5578] [INSPIRE].

[54] P.B. Arnold, *Simple Formula for High-Energy Gluon Bremsstrahlung in a Finite, Expanding Medium*, *Phys. Rev.* **D 79** (2009) 065025 [arXiv:0808.2767] [INSPIRE].

[55] P.B. Arnold and W. Xiao, *High-energy jet quenching in weakly-coupled quark-gluon plasmas*, *Phys. Rev.* **D 78** (2008) 125008 [arXiv:0810.1026] [INSPIRE].